2023

THE IMPACT OF CHANGING SHIPPING EMISSIONS ON THE ATMOSPHERIC DEPOSITION OF TRACE ELEMENTS AND SULFUR TO THE WESTERN ENGLISH CHANNEL AND COASTAL ZONE

Windell, Laurence Christian

https://pearl.plymouth.ac.uk/handle/10026.1/20620

Copyright Statement

THE IMPACT OF CHANGING SHIPPING EMISSIONS ON THE ATMOSPHERIC DEPOSITION OF TRACE ELEMENTS AND SULFUR TO THE WESTERN ENGLISH CHANNEL AND COASTAL ZONE

by

LAURENCE CHRISTIAN WINDELL

A thesis submitted to the University of Plymouth

in partial fulfilment for the degree of

RESEARCH MASTERS

School of Geography, Earth and Environmental Science

[In collaboration with Plymouth Marine Laboratory]

February 2022

<u>Acknowledgements</u>

Author's Declaration

At no time during the registration for the degree of Research Masters has the author been registered for any other University award without prior agreement of the Doctoral College Quality Sub-Committee.

Work submitted for this research degree at the University of Plymouth has not formed part of any other degree either at the University of Plymouth or at another establishment.

Contributed to the ACRUISE project (Plymouth Marine Laboratory).

Conferences:

International Aerosol Conference 2022, Athens, Greece, 4-9 September 2022 (poster presentation):

"The impact of the IMO-2020 shipping regulation on the atmospheric deposition of sulfur around the Western English Channel and the use of the V/Ni ratio as a shipping marker"

Czech Aerosol Society Conference 2022, Kutna Hora, Czech Republic, 2-10 October 2022 (15-minute oral presentation):

Recipient of Dekati Young Scientist Award

"The impact of the IMO-2020 shipping regulation on the atmospheric deposition of sulfur around the Western English Channel and the use of the V/Ni ratio as a shipping marker"

Word count of main body of thesis: 15065

Signed: Laurence Christian Windell

Date: 21/03/2023

Table of Contents

Abstract

Laurence Christian Windell - The impact of changing shipping emissions on the atmospheric deposition of trace elements and sulfur to the western English Channel and coastal zone

Maritime shipping is a significant source of anthropogenic emissions, with annual growth of shipping continually on the rise. In the marine environment, shipping emissions often dominate the atmospheric deposition of sulfur and contribute significantly to global sulfur emissions. As a result, the International Maritime Organisation (IMO) introduced a regulation on 01/01/2020 restricting global marine fuel sulfur content from 3.5% to 0.5% w/w.

The present study investigated the changes in airmass marine aerosol chemical character arriving at the Penlee Point Atmospheric Observatory (PPAO; 50°19′N, 4°11′W) to gain insight into the efficacy of the IMO-2020 regulation. The observatory in Southwest England is ideally located next to the port of Plymouth and near to a major international shipping lane in the English Channel with high density marine traffic. Aerosol filter samples were collected from 2020-2021 (n=64). Filter samples were water-leached and subsequent leachates were analysed for major ions using Ion Chromatography, and trace elements using Inductively Coupled Plasma – Mass Spectrometry. Concentrations of V/Ni and calculated non-sea-salt sulfate (nss-SO_4^{2-}) were compared to PPAO datasets from 2015-16 and 2017-18 respectively.

The vanadium/nickel (V/Ni) ratio has been widely used as a marker of shipping emissions in the marine boundary layer, with the range of 2.5 to 4 indicating shipping activity. Trace element analysis showed a drop in V from 2.91 pmol/m^3 to 1.44 pmol/m^3, and Ni increase from 0.95 pmol/m^3 to 4.8 pmol/m^3. V/Ni ratio post-IMO-2020 decreased from 3.3 to 0.28, showing a significant change to the trace metal signature of marine aerosols.

7

Post-IMO-2020 nss-SO_4^{2-} concentrations were significantly lower than pre-IMO-2020 values (n=109, p<0.05), with total nss-SO_4^{2-} concentration dropping from 1.35 µg/m^3 to 0.33 µg/m^3. A change from nss-SO_4^{2-} dominated atmospheric sulfur pre-IMO-2020 to primarily natural dimethylsulfide dominated sulfur was observed. Clear seasonal nss-SO_4^{2-} fluctuations increasing during spring and summer were visible post-IMO-2020.

These results indicate a major change to the atmospheric chemistry of sulfur in the lower atmosphere near to regions of intense shipping.

List of Figures

List of Tables

The impact of changing shipping emissions on the atmospheric deposition of trace elements and sulfur to the western English Channel and coastal zone

<u>Chapter 1. Introduction</u>

Anthropogenic aerosols have a significant impact on marine ecosystems and human health, with the shipping industry contributing as a source of these emissions. New global restrictions on marine sulfur emissions have been implemented to bring about a reduction in these emissions. However, the resultant change in atmospheric emissions has an unknown effect on the environment (Halff et al., 2019, Ji, 2020). The International Maritime Organization (IMO) 2020 regulation restricts the sulfur content in marine fuels globally, from its original value of 3.5% to 0.5%, and 0.1% when used in Emission Control Areas (ECAs) (IMO, 2019). In addition, reductions in shipping activity during the COVID-19 pandemic had a measurable impact on shipping emissions (March et al., 2021, Millefiori et al., 2021, Verschuur et al., 2021). Shipping emissions often dominate the atmospheric deposition of sulfur in the marine environment and are a prominent source of emissions of vanadium (V) and nickel (Ni) (Aksoyoglu et al., 2016, Chen et al., 2019, Cheng et al., 2019). Emissions of sulfur and their effect on the environment and humans have been widely studied and there is significant evidence of their contribution to acid rain and ocean acidification, as well as respiratory and cardiovascular diseases in humans (Qian et al., 2019, Yang et al., 2009).

1.1   <u>Marine Aerosol</u>

Marine aerosols constitute all airborne particles found over the ocean, and their characteristics are contributed to by numerous natural and anthropogenic sources, with the largest contributor being produced mechanically at the ocean surface (Saltzman, 2009). Marine aerosols greatly

affect the Earth's atmosphere and radiative forcing, influence air quality, and consequently affect marine ecosystems (O'Dowd et al., 2007, Saltzman, 2009). Marine aerosols are usually found in three modes based on size: the Aitken mode (<0.1 µm), the accumulation mode (0.1 - 1 µm) and the coarse mode (>1 µm (Chester, 1990, Saltzman, 2009). However, aerosol fractions overlap, with some classifications found as i) fine fraction (<2.5 µm) and coarse fraction (>2.5 µm), or ii) fine fraction (1 µm) and coarse fraction (>1 µm). The main marine aerosol characterised groups are found in Table 1.1.

Table 1.1. Composition and sources of common aerosols found in the marine atmosphere. Sea salt is often the dominant aerosol by weight, while other aerosols outlined vary based on locality and influence of anthropogenic emission sources (Chen et al., 2018, Koulouri et al., 2008, O'Dowd et al., 2004; 2007, Saltzman, 2009).

Aerosol	Major chemical components	Main Sources
Sea salt (dominant)	NaCl, SO_4^{2-}, K^+, Mg^{2+}, Ca^{2+}, organic matter	Sea spray (mechanical production)
Non-sea-salt sulfate	nss-SO_4^{2-}	Dimethyl sulfide (DMS) production, volcanoes and fossil fuel combustion
Nitrate	NO_3^-	Fossil fuel combustion, biomass burning
Carbon-based	Various carbon compounds	Fossil fuel combustion, biomass burning/wildfires, sea surface

1.2 Sulfur

Sulfur (S) is a non-metallic element belonging to group 16 of the table of elements, has an atomic number of 16, and is the 5th most abundant element on Earth. Sulfur plays a large role in the marine environment and is commonly found in the atmosphere and hydrosphere. It is essential for all life as a macronutrient and needed for the normal function of organisms (Madigan et al., 2015). The element is used in microbial respiration, the production of proteins and enzymes in plants and animals, and is an essential element in the amino acids cysteine, methionine and taurine in humans, as well as helping to prevent diseases (Hill et al., 2022). The element is found in many marine aerosols and gases, tracing back to both natural and anthropogenic sources (Gray et al., 2011). The 2016 Air Pollution Report by the International Energy Agency found fossil fuel combustion to be the leading source of atmospheric sulfur dioxide emissions (IEA, 2016).

1.3 Marine Sulfur Cycle

The ocean is a reservoir of sulfur and contributes to the chemical makeup of marine aerosols. The three main emission pathways providing sulfur in the marine environment are: (1) the production of DMS, formed by the oxidation of dimethlysulfoniopropionate (DMSP) produced by marine phytoplankton, (2) the emission of anthropogenic SO_x and (3) the sea-salt aerosol (SO_4^{2-}), produced mechanically by the bursting of bubbles at the sea-surface interface upon the crashing of waves (Chen et al., 2018, Saltzman, 2009).

DMS production and anthropogenic sulfur emissions are classed as non-sea-salt sulfate (nss-SO_4^{2-}) aerosols. These are aerosols not produced by sea water droplets, and must be distinguished from sea-salt aerosols in order to investigate contributions to marine atmospheric sulfur. Nss-SO_4^{2-} is calculated through a subtraction of sea-salt sulfate using the standard ratio of sodium to sulfate concentration in sea water, and in theory, with only nss-SO_4^{2-} remaining.

A fraction of DMS passes through the ocean layer into the air and is oxidized by OH^- and NO_3^- forming methane sulfonic acid (MSA) (Fung et al., 2022).

Anthropogenic nss-SO_4^{2-} can be identified by concentrations of trace species. V and Ni concentrations are an important marker of marine anthropogenic sources, due to their content in unregulated marine fuels (Prospero, 2002). Sea-salt aerosol characteristics are, by definition, directly related to the seawater from which it was produced and therefore, easily distinguished by high sodium and magnesium content (Prospero, 2002, Saltzman, 2009). The sea-salt aerosol is one of the aerosols found in the highest concentrations in the marine environment.

1.4   Shipping Emissions: Sulfur and Particulate Matter

Anthropogenic marine sulfur emissions are most commonly released through the combustion of fuel oils, which have been known to contain up to 6% w/w sulfur content until regulation changes during the last two decades (Jasińska et al. 2012). During the combustion stage, commonly used heavy fuel oils (HFOs) release sulfur, which is then oxidised in the atmosphere into SO_2, later reacting in the atmosphere and converting to SO_3 and SO_4^{2-} (Pirjola et al., 2014). For simplicity, the sulfur pollutants emitted are referred to as SO_x. Maritime emissions of SO_x are directly correlated with the production of particulate matter (PM), of which sulfate (SO_4) is a major component (Lv et al., 2018). PM is often released as secondary formation from fuel combustion, in the sizes of PM_1 (less than or equal to 1µm), $PM_{2.5}$ (less than or equal to 2.5µm) and PM_{10} (less than or equal to 10µm). PM is found as a mixture of liquid and solid particles containing a variety of pollutants including sulfate and metals (Furger et al., 2017).

Shipping SO_x and PM emissions heavily affect the chemistry of the atmosphere and thus air quality, particularly on a regional scale. Around 70% of shipping activity is carried out within 400 km of the coast, highlighting its effect on air quality in these regions (Corbett et al., 1999, Eyring et al., 2010). Research showed that emissions can cause as much as 75% of nss-SO_4^{2-}

in coastal areas where anthropogenic and shipping are major contributory factors (Schulze et al., 2018).

The production of sulfur dioxide (SO_2) from the combustion of fossil fuels has had major environmental impacts and sulfur emissions from the shipping industry are of great concern due to their effect on air quality. The widespread effects of shipping emissions have led to it being extensively investigated. The industry contributes heavily to global SO_x emissions, with 11.3 million tonnes of SO_x emitted annually between 2007 and 2012 (IMO, 2014). This value represented 13% of global SO_x emissions. In addition, ship emissions also accounted for 15% of global NO_x emissions.

Aside from NO_x and sulfur oxides (and of course CO_2), ships also emit fly ash, soot and quantities of trace metals, such as V and Ni, which are associated with PM. Annual global shipping emissions of NO_x, SO_x and PM are presented in Figure 1.1 and show the consistent emissions of SO_x and PM from 2007 to 2015, with NO_x appearing to decrease slightly. Pre-2020 emission regulation implementation, the most commonly used marine fuel was HFO, which is high in sulfur, V and Ni.
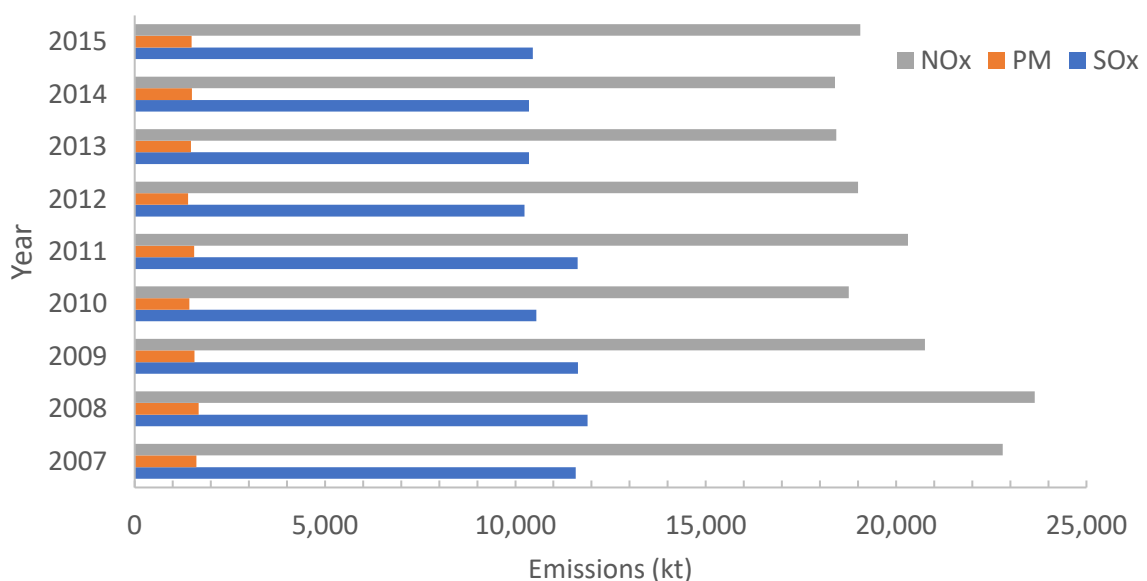
Figure 1.1. Yearly global shipping emissions of NO_x, SO_x and PM (ICCT, 2017, IMO, 2014)

1.5 Studying transboundary transport of aerosols

When evaluating areas affected by shipping emissions, the transboundary transport of aerosols must be taken into consideration. Shipping emissions do not only affect coastal communities; the long-distance transport of shipping-related aerosols means that areas up to 960 km from the source can be affected (Lv et al., 2018). Transboundary transport of aerosols is heavily dependent on meteorological conditions and therefore the affected areas vary. Wind speed and direction greatly influence the transport of aerosols. The Hybrid Single-Particle Lagrangian Integrated Trajectory (HYSPLIT) model is often used as a user-friendly open source tool to determine aerosol trajectories and thus identify their sources. Using the HYSPLIT model, SO_2 emissions from central and eastern Europe have been found to heavily affect the sulfate concentrations in the eastern Mediterranean (Rudich et al., 2008). Central Chinese aerosol emissions have been shown to have a significant effect on South Korean aerosols during periods of high pollution (Lee et al., 2019); in fact, travel distances of air masses were found to be over 750 km/day. Many studies highlight the importance of wind direction on the transboundary transport of air masses, using evidence of long-range transport of aerosols over long distances, including between different continents (Hongisto et al., 2004, Kim et al., 2012, Kindap et al., 2006, Lin et al., 2005).

On local spatial scales, examples of models can be found for impact of individual vessels. Streets et al. (1997) studied SO_2 concentrations around a 12 kt ship using 3.3% sulfur oil (under 6m/s wind speed). Air concentrations were recorded as 64 $\mu g/m^3$ at 2.5 km distance from the ship and 10 $\mu g/m^3$ at 20 km, suggesting the effects of ship emissions are greater on a local scale (Streets et al., 1997).

1.6   <u>Shipping contribution to SO_x and PM</u>

There is extensive research on the contribution of the shipping industry to SO_x and PM emissions (Aksoyoglu et al., 2016, Beecken et al., 2014, Chen et al., 2019, Cheng et al., 2019, Corbett et al., 1999, Dore et al., 2007, Lv et al., 2018, Pirjola et al., 2014, Schulze et al., 2018, Streets et al., 1997, Yang et al., 2016, Yeeles, 2018, Zhang et al., 2014, Zhao et al., 2013). With increasing global demand for products and sea transport, fuel consumption has steadily increased over the last century (Johansson et al., 2017, Øyvind et al., 2007). By the year 2000, annual cargo transport was at 5.4 Mt, a number 18 times larger than in 1920 (Øyvind et al., 2007). With this increase in transport comes a drastic increase in SO_2 emissions, with a reported 8.5 Tg SO_2 emitted in 2000. Just 17 years later, annual SO_2 emissions grew to 20.88 Tg, which accounted for 9% of global SO_2 emissions for that year (Chen et al., 2020). IMO regulations have come at a crucial time, as global demand for products is continually increasing, leading to greater rates of atmospheric sulfur deposition.

Coastal areas prove excellent study sites to monitor shipping emissions and also investigate their effects on the environment. However, due to the long-range transport of aerosols, affected areas can include those far from shipping activity. Using the UK as an example, shipping-related European SO_2 emissions heavily contribute to acidification of ecosystems (such as rivers, forests and lakes), pointing towards the value of international policies (Dore et al., 2007). A study modelling SO_2 emission rates in the UK calculated that with shipping emissions increasing by 2.5% annually, the resultant contribution to average sulfur deposition in the area would increase to 28% from 9% between the years 2002 and 2020 (Dore et al., 2007).

A good example of ship-related emissions in an area of high marine traffic are the shipping lanes of the Mediterranean. Aksoyoglu et al., 2016 reported ship traffic contributed to 45% of $PM_{2.5}$ concentrations in the Mediterranean Sea while in the Baltic Sea, values were up to 15%. Shipping in the Mediterranean was found to be responsible for 49% of SO_x emissions in Europe

(Jalkanen et al., 2016), highlighting the contribution of shipping to total anthropogenic SO_x emissions. A North Sea study of 4 Belgian ports had similarly high values of 31 kt SO_x between 2003 and 2004, making up 30% of all emissions in Belgium. Further research on the Baltic Sea found shipping emissions to represent ~80% of local SO_2 emissions in some areas (Claremar et al., 2017). Meanwhile in Europe, research using automatic identification system (AIS) found total annual European emissions of SO_x and $PM_{2.5}$ in 2011 to be 1200 and 200 kt respectively (Jalkanen et al., 2016).

Two Spanish studies both found 4% ship related PM_{10} increases over background levels, with the first also finding 14% $PM_{2.5}$ increases (Querol, 2001, Viana et al., 2009). In Turkey, studies found high values of SO_x and PM emissions from ships; for example, Deniz and Durmuşoğlu (2008) report over 87 kt SO_x and 4.7 kt PM emitted per year in one of Turkey's main ports. Saraçoğlu et al. (2013) found similar values of SO_x at 83 kt, while their PM emissions were lower at 165 t. However, the lack of percentage contribution of shipping towards total area emissions proves problematic when comparing with studies from other areas. A study on the area of water 200 km around the whole coastline of the Australian region, high in marine traffic, produced shipping-related SO_x and PM values of 115 and 15 kt/year respectively (Goldsworthy et al., 2015).

Asia is a region in which intense ship traffic heavily affect inland and coastal communities. Extensive studies on the emissions of SO_2 and $PM_{2.5}$ in the area have been conducted (Chen et al., 2019, Ding et al., 2019, Fan et al., 2016, Ma et al., 2019, Zhang et al., 2014, Zhao et al., 2013). In China, shipping-related emissions can contribute up to 30% of $PM_{2.5}$ emissions in megacities during periods of ship-plume transport (Lv et al., 2018). Lv et al. (2018) conducted a study almost 400 km away from the coast of China, in which 918 kt SO_2 and 119 kt PM were found to be emitted by shipping activities per year, representing 20% of total SO_2 emissions in a heavy industrial area. They also found that within 22 km, shipping emissions accounted for

up to 56% of total SO_2 emissions. Shipping-related emissions of SO_2 and $PM_{2.5}$ in the Yangtze River Delta port cluster, 400 km from the coastline, were determined to be an average of 165 kt and 51 kt per year with shipping providing 43.5% of SO_x emissions in the area. It was shown that 65% and 80% of initial emissions occurred inland at 100 km and 200 km respectively, with SO_2 emission values from ships being 36 times greater than land-sourced emissions (Fan et al., 2016).

1.7 Trace elements

V and Ni are the most abundant trace metals found in HFOs and are subsequently used as markers of marine anthropogenic fuel combustion. V and Ni are usually found as oxides and are vaporised during the combustion stage, being released in PM (Corbin et al., 2018). V and Ni are also detrimental to ship integrity due to their corrosion of exhausts. In addition, both metals are considered hazardous substances and are toxic to humans (Spada et al., 2018, Visschedijk et al., 2013). Globally, 200 million kg V are emitted by human activities per year, compared to 65 million kg V naturally released from dust and volcanic eruptions (WHO, 2000). A significant source of V is the burning of crude or residual oil. V is present in HFOs in concentrations of up to 100s of mg/kg, while Ni is usually found to be approximately one tenth of V concentrations (Spada et al., 2018, Visschedijk et al., 2013). In North-West Europe in 2005, a total of 1570 t V were emitted, 39% of which were due to the shipping industry (Visschedijk et al., 2013).

Due to V and Ni being the most abundant trace metals emitted from HFO burning ships, other toxic metals are less studied (Corbin et al., 2018, Zhao et al., 2021). This is usually since they are not used as shipping-specific markers and are also released by inland industries (Zhao et al., 2021). Other trace elements of interest include chromium, lead, aluminium, iron, arsenic, and manganese due to the potential threats they pose to the environment (Jahan et al., 2019).

Depending on their solubility, trace metals can leach from PM into the ocean, causing a threat to aquatic life in high concentrations (Ansari et al., 2004). Trace metals are found in deep ocean waters, with their solubility often varying with depth, based on salinity and interactions with particles (Aparicio-González et al., 2012). A review on ocean and surface water metal concentrations showed Cd, Cu, Ni and Zn being found up to ca 0.8, 11, 10 and 10 nmol/l at 6000m, showing increasing concentrations with depth (Aparicio-González et al., 2012). Hence, although difficult to quantify, the contribution of trace metal pollution by ships must be considered.

1.8   Techniques for quantification and estimation of shipping emissions contributions

Estimating shipping emissions on a global scale proves difficult due to the abundance of anthropogenic emissions from varying sources. A common method is to produce sulfur inventories using emission data from ships, and calculating emission values based on fuel types (Corbett et al., 1999). The use of AIS has become a useful tool in producing shipping emission inventories, as it allows for the tracking of ships (Chen et al., 2017, Li et al., 2016). This high-resolution technique can produce accurate regional estimates of shipping emissions for SO_x and PM and can quantify emissions from separate vessel types.

Li et al. (2016) used AIS to assess shipping emissions in the Pearl River Delta (PRD) region in China, estimating SO_2, PM_{10} and $PM_{2.5}$ emissions in 2013 to be 61.4, 7.1 and 6.6 kt respectively (Li et al., 2016). The study assessed varying vessel types and attributed the majority of emissions to cargo and container ships. The system also highlighted emission hotspots, providing excellent information in terms of emission control methods. A comparable study including the same area as a sample site a year later showed similar results (Chen et al., 2017). The same vessel types were attributed to the bulk of shipping emissions and, in addition, it was

noted that the PRD region accounted for 17% of national Chinese shipping emissions out of a total of 1193 kt.

1.9 Aerosol trace metal ratios as indicators of shipping

Due to their high abundance in HFO, ratios of V/Ni have been used when analysing aerosols as markers of shipping emissions. The ratios can be used to identify sources of emissions and they are representative of the type of fuel used (Ogunlaja et al., 2014, Viana et al., 2009, Yakubov et al., 2016). The widely-accepted V/Ni range for shipping emissions is between 2.5 and 4, confirmed through studies on exhaust stacks (Chianese et al., 2022, Mazzei et al., 2008, Nigam et al., 2006, Viana et al., 2009). However, ratios may vary based on different fuel oils. For example, for light, medium and heavy crude oils, a study found V/Ni ratios to be 0.47, 1.36 and 2.77 respectively (Ogunlaja et al., 2014). In shipping emissions studied at a Mediterranean harbour in a SECA (Sulfur Emission Control Area) (Melila, Spain), PM_{10} and $PM_{2.5}$ had V/Ni ratios of 4-5 (Viana et al., 2009).

A study on heavy oils found V and Ni concentrations between 0.0049 and 0.1795 wt%, and a total concentration of V and Ni in asphaltenes of up to 1 wt% (Yakubov et al., 2016). Zhao et al. found ship-related emissions of V and Ni found in $PM_{2.5}$ of 80 and 14.8 ng m $^{-3}$, conducted in Shanghai port (Zhao et al., 2013). Pey et al. found V, Ni and Cd values in a port up to 75% higher when compared to urban areas, with these values being attributed mostly to shipping (Pey et al., 2013).

Owing to the impact of V and Ni concentrations from other combustion sources, using the V/Ni ratio as an identifier of shipping emissions is complex (Viana et al., 2009). The method becomes problematic when sampled in a region near urban and industrial areas.

1.10 Sampling and analytical methods of airborne particulate matter

In-situ measurements entail filtration systems using air pumps and sample filters (often quartz, polycarbonate or glass) to collect aerosol samples for laboratory analysis. Water-soluble fractions of aerosols collected from filters can be extracted using double distilled/high purity water to investigate readily leachable constituents, while acid digests investigate total metal concentrations (Chandra Mouli et al., 2003, Tolocka et al., 2001). In the case of water-solubility of V and Ni emitted through anthropogenic sources, Cascade impactors are often used to determine aerosol particle size, allowing for the analysis of size classified aerosols such as $PM_{2.5}$ and PM_{10}.

Passive sampling and analysis can be used for the continuous measurements of ambient air. Aerosols pass through a PM head, allowing for particles of a specific size, and are deposited onto a substrate; microscopy is then used to determine particle number and size (Alemón et al., 2004, Byeon et al., 2015). A new technology, the Xact Ambient Metals Monitor, offers online, continuous measurements of aerosol composition (Furger et al., 2017). Aerosols are collected on a filter tape and subsequently analysed using X-ray Fluorescence without destroying the sample, as is the case with ion chromatography (IC) and inductively coupled plasma-mass spectrometry (ICP-MS).

Instrumental Neutron Activation Analysis (INAA) is often used to characterise air filters. Neutrons are bombarded onto the sample creating radioactive isotopes, whose gamma rays are subsequently measured, with the ability to analyse samples with very little mass (Ott et al., 2008). The method does not destroy the sample and is found to be competitive with ICP-MS in terms of sensitivity and detection limits, depending on element analysed.

Further, Ion Chromatography is a popular method used to analyse multiple major ions within aerosol samples due to its high sensitivity, low limit of detection, and simple sample

preparation (Fosco et al., 2007). It is used to separate, identify and determine chemical character of complex mixtures and is greatly effective in analysing major ions from aerosols (Chandra Mouli et al., 2003). Samples are introduced to the IC system to analyse ions and cations using respective eluents. For anion eluents, carbonates such as $NaHCO_3$ or Na_2CO_3 can be used; for cations, oxalic acid $C_2H_2O_4$ or tartaric acid $C_4H_6O_6$ can be used (Chandra Mouli et al., 2003, Fosco et al., 2007). Resulting chromatograms and their peaks are analysed, determining their peak height and area in order to extrapolate element concentration within the sample.

As previously mentioned, low detection limits of IC make the method very favourable. For sulfate, the modern limit of detection and limit of quantitation for Thermo Scientific^{TM} Dionex^{TM} ICS-5000$^+$ HPIC^{TM} IC System are reported as 0.013 and 0.04 mg L^{-1} respectively (Basumallick, 2016). To reduce error and increase accuracy, filter blanks are determined by analysing clean filters and process blanks (filters exposed to the same procedure as samples). The resulting sample ion concentrations are subtracted from background filter values.

Inductively Coupled Plasma Mass Spectrometry is a highly accurate and sensitive analytical technique, often used to detect elements in trace concentrations. The system works by ionizing samples, creating small ions, which are subsequently accelerated in a vacuum and detected; and their masses measured. The technique is widely used in environmental analyses due to extremely low detection limits (up to parts per trillion), wide dynamic linear range, the ability to analyse for multiple elements in a short time, good precision and low sample quantity use (Lu et al., 2020, Wysocka, 2021).

Another technique, Inductively Coupled Plasma Optical Emission Spectroscopy (ICP-OES), is also used for elemental analysis. Instead of measuring mass such as in ICP-MS, the light from excited atoms and ions are determined for the respective elements. ICP-OES boasts detection

limits up to ppm and is often used for samples containing dissolved solids, such as soil and water samples (Chojnacka et al., 2018).

1.11   Impact of shipping emissions on the environment

SO_2 emissions are linked to various environmental effects; one being acid rain which can be formed by the reaction of either SO_2 and NO_x with water and oxygen, leading to the formation of sulfuric and nitric acid respectively (EPA, 2019). The formation of acid rain leads to acidification of oceans and soils, subsequently damaging forests and crops, and although regulations reducing SO_2 emissions such as the National Emission Ceilings Directive have been in place since 1990, its effects are still persistent in areas such as China (Huang et al., 2019, Ji-ming et al., 2000, Likus-Cieślik et al., 2020, Yun et al., 2019). As for ocean acidification, a significant proportion of the acidity can be attributed directly to the shipping industry (Chen et al., 2018, Claremar et al., 2017, Gray et al., 2011, Im et al., 2013). While in general, CO_2 plays a greater role in ocean acidification, SO_x has an almost equal role in areas of high marine traffic (Hassellöv et al., 2013).

The ocean is a sink of atmospheric gases and, depending on air chemistry, these gases can enter the ocean via exchange through the air-sea interface (Chester, 1990). High sulfur content in the air results in molecular diffusion or mechanical mixing of SO_x into the ocean, greatly affecting ocean chemistry and thus marine life. The air-sea gas exchange is also responsible for the transfer of dimethylsulfide (DMS) from the ocean to the air (Uher, 2006). Diffusion rates depend on sea and air sulfur concentrations. Wind speed is also an important factor controlling diffusion rates since bubbles formed by crashing waves deposit atmospheric particles into the ocean. Bubbles can travel up to a depth of 20 m during periods of high winds and the high pressure at this depth increases total gas exchange (Chester, 1990).

Metals dissolved in seawater or in particulate form have toxic effects on marine biota (Mahowald et al., 2018). Their toxic effects include disruption of reproductive systems, inhibition of growth and birth defects, and the potential to bioaccumulate and affect the entire trophic chain (Mahowald et al., 2018). One example of this is a study on a species of oysters in a busy seaport. Used as a bioindicator, the species was found to have significantly higher levels (up to 5 times greater) of trace elements such as Pb, Cu and Zn over background levels, highlighting possible pollution released by shipping activity (Jahan et al., 2019).

Aerosols play an important role in climate forcing due to their cloud interactions Aerosols, such as sulfate, increase droplet concentration in the atmosphere and affect liquid water content, thickness and lifetime of clouds, resulting in a change of the Earth's radiation budget in the direction of climate cooling (Lohmann, 2006). Shipping emissions thus have direct effects on climate change, as outlined in a study which found that shipping-originated aerosols increased local aerosol optical death from 20% to 36% in China (Xie et al., 2019).

1.12 Impact of shipping emissions on human health

Inhalation of SO_2 can have serious adverse health effects in humans (Carmichael et al., 2002, Chen et al., 2012, Curtis et al., 2006, Goudarzi et al., 2016, Greaver et al., 2012, Kampa et al., 2008, Yang et al., 2009). SO_2 can cause respiratory irritation, bronchoconstriction, heart rate abnormalities and pulmonary and cardiovascular diseases (Chen et al., 2012, Curtis et al., 2006, Tunnicliffe et al., 2001, Yang et al., 2009). Furthermore, SO_2 aggravates pre-existing lung and heart conditions such as asthma, and is strongly correlated with atopy, especially in children (Rosser et al., 2020). Shipping emissions can cause an estimated ~14 million child asthma cases per year stemming from SO_2 and PM emissions (Sofiev et al., 2018). SO_2 concentrations of 200ppb have been shown to cause changes in lung function (Tunnicliffe et al., 2001). Of subjects exposed to high SO_2 levels (>100ppm) in a working environment, 64% showed signs

of restrictive lung disease (Soeroso et al., 2019). Likewise, reduced lung power in asthmatic subjects were observed at 200 ppb SO_2, a concentration often observed in Europe during periods of high air pollution (Anderson et al., 1997). On the whole, air pollution from PM (including NO_x, SO_2 and VOCs) is estimated to cause from 400,000 to 800,000 premature deaths per year (Chu Van et al., 2019, Curtis et al., 2006). A summary of common pollutants and their relevant health effects on humans are shown in Table 1.2.

Table 1.2. Common shipping emission pollutants and their effects on humans

Pollutant	Human effect	Reference
SO_x	Respiratory disease and irritation, pulmonary and cardiovascular diseases and premature deaths.	(Chen et al., 2012, Curtis et al., 2006, Goudarzi et al., 2016, Kampa et al., 2008)
Cu	Respiratory and liver disease.	(Amoatey et al., 2019)
V	Cardiovascular morbidity and respiratory diseases.	(Amoatey et al., 2019, Lin et al., 2018)
Ni	Carcinogenic. Cardiovascular and cerebrovascular morbidity.	(Amoatey et al., 2019, Lin et al., 2018)
Cd	Carcinogenic. Lung and cardiovascular disease.	(Nordberg et al., 2018)
Cr	Carcinogenic. Respiratory irritation.	(Pavesi et al., 2020)
As	Carcinogenic. Cardiovascular, liver and kidney diseases.	(Amoatey et al., 2019, Jomova et al., 2011)
Pb	Premature deaths, kidney and brain damage.	(Assi et al., 2016)

The inhalation of PM with associated trace metals are directly linked to lung, bladder and skin cancer, with PM_{10} and $PM_{2.5}$ having high deposition rates onto the lungs (Amoatey et al., 2019). The number of life years lost due to the inhalation of anthropogenic $PM_{2.5}$, with predictions up to 2050, are seen in Figure 1.2. Calculations were made using a Current Legislation Projection based on future policies and those already in place. With the most abundant metals in HFOs being V and Ni, their effects on humans must be considered. Exposure to V can cause acute and chronic respiratory effects and has also been associated with depression and Parkinson's disease (WHO, 2000). At low concentrations of exposure, it causes coughing, irritation of the respiratory tract and changes in parameters of lung function. At higher concentrations of exposure, serious respiratory irritation and frequent coughing are observed (WHO, 2000). V and Ni concentrations in $PM_{2.5}$ from shipping emissions were associated with cardiovascular mortality, and Ni was associated with cerebrovascular mortality (Lin et al., 2018). Other trace metal such as cadmium, chromium, arsenic, lead and copper, which are often released from HFOs (initially at high concentrations), can also greatly harm human health through their inhalation threat, most of which are carcinogens (See Table 1.2) (Lee et al., 1973). Lead and arsenic have been linked to premature births and birth defects, cadmium causes bronchitis and pulmonary irritation, while cadmium and copper are known to cause lung disease (Amoatey et al., 2019).
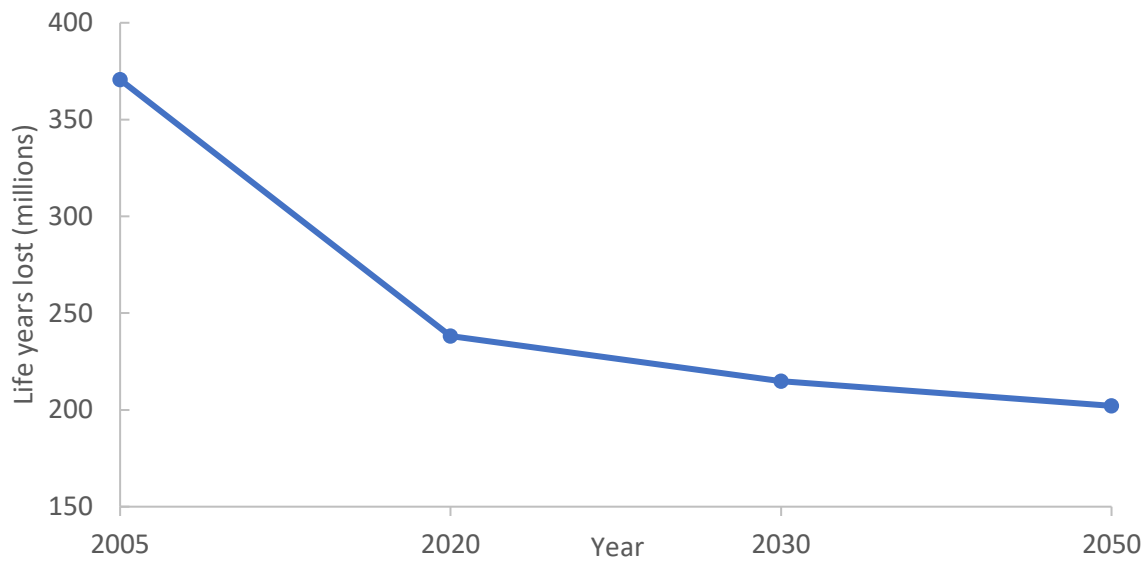
Figure 1.2. Annual life years lost due to anthropogenic PM$_{2.5}$ in the EU (Campling, 2013).

1.13   Shipping Regulations

The IMO is a UN body governing global shipping. IMO regulations controlling the environmental impact of shipping have been in place since 1983 (IMO, 2019). In 1973, the International Convention for the Prevention of Pollution from Ships (MARPOL) came into being. MARPOL Annexes I-VI covered the prevention of pollution through oil and wastewater discharges, release of garbage and harmful substances, and air pollution. From 2005, in accordance with the MARPOL Annex VI, regulation of NO$_x$, SO$_x$ and Volatile Organic Compounds (VOCs) were required as well as introducing ECAs in which sulfur fuel content limits were capped at 1.5% (George et al., 2017). The ECAs include the North Sea, Baltic Sea and the coasts of the US, as well as recently implemented zones around China.

More recently, IMO-2020 regulations implemented strict SO$_x$ emission limits, introducing the need to use low-sulfur fuel oils and/or the use of exhaust gas cleaning systems (ECGS) (Kontovas, 2020). Table 1.3 details IMO changes to SOx emissions for ECAs and Open Ocean areas.

Table 1.3. International regulation changes on SO_x (IMO, 2014)

Global SO_x emission limit	SO_x emission limit within ECAs
4.5% before January 2012	1.5% before July 2010
3.5% before January 2020	1% before January 2015
0.5% post January 2020	0.1% post January 2015

The regulation IMO-2020 was implemented on 1 January 2020, requiring marine fuels to contain no more than 0.5% sulfur, from its previous limit of 3.5% (with a limit of 0.1% in SECAs) (IMO, 2019). Due to this regulation, changing practices were needed to meet the new sulfur cap. This included changes in fuel types, engine types and the implementation of new technologies. In ships that continued to use HFOs, EGCS (also known as 'scrubbers') must be fitted to meet the required sulfur emissions limit.

Despite the lack of regulations specifically controlling the emission of trace metals from ships, a further potential positive effect of IMO-2020 is the reduction of heavy metals emissions. Low-sulfur fuels contain significantly lower trace metal contents and the large-scale use of these fuels to meet sulfur emissions limits as required by IMO-2020 is predicted to reduce V/Ni emissions (Spada et al., 2018, Xiao et al., 2018). When switching from HFO to Marine Gas Oil (MGO), concentrations of V reduced from 100 ± 47 ppm to under 1ppm (Tao et al., 2013). Upon implementation of a 2009 sulfur emission regulation in a Californian ECA, reducing shipping fuel sulfur content below 1.5%, V emissions reduced between 28-64% across 6 samples sites, correlated with the reduction in SO_2 emissions of up to 72% (Tao et al., 2013). Further, Kotchenruther et al. (2015; 2017) conducted two studies in the US investigating sulfur regulations and found V and Ni emissions to be significantly reduced by 29-65%. This reduction correlated with reduced $PM_{2.5}$ emissions that was directly related to the phasing out

of HFOs. Another study in the US found that annual mean V concentrations in the major ports of Seattle and New Orleans decreased by 35% and 85% after the implementation of the 2015 SECA capping marine fuel sulfur content at 0.1%, bringing the concentrations closer to inland values (Spada et al., 2018). The study also noted similar reductions in Ni for the same sample sites.

1.14   Effects of ECAs and IMO regulations

The implementation of the IMO-2020 sulfur cap is predicted to have positive effects on the environment though it could, ironically, lead to an increase in global warming (George et al., 2017, Halff et al., 2019, Ji, 2020, Mattson, 2006, Svensson, 2011). However, positive effects will include higher air quality, reductions in acid rain production, reducing environmental damage as well as reducing the number of deaths due to SO_x and PM emissions (Ji, 2020). The increased air quality will greatly benefit coastal communities in close contact with marine traffic, in addition to inland communities which are affected by the long-distance transport of ship-related aerosols.

The IMO predicted a reduction in shipping-related SO_x emissions after the implementation of IMO-2020 of 77% compared to pre-2020 values (IMO, 2016). The main measured contributors to lower air quality are SO_x and PM emissions, therefore, a decrease in these emissions should have a noticeable impact after the IMO-2020 regulations are adhered to. The IMO's 2016 investigation into the possible effects of its 2020 regulations predicted strong results. Through the first 5 years of its implementation, annual sulfur emissions were projected to decrease by 8.5-8.9 Mt (IMO, 2016). Another study by Sofiev et al. (2018) estimated a decrease in SO_x and PM emission of 75.5% and 45%, respectively, post IMO-2020 compared to 2012 values calculated during the third IMO GHG study (seen in Table 1.4). The same study also predicted a decrease in premature deaths of 266,300 (a reduction of ~34%), as well as a reduction of 7.5

million child asthma cases, compared to values prior to the implementation of IMO-2020. The majority of adult mortality reductions (80%) due to low-sulfur regulations will affect Asia, whereas the reductions in child mortality rates will mostly affect Asia and Africa (54% and 33% respectively) (Sofiev et al., 2018).

Table 1.4. Annual shipping-related pollutant emissions of SO_x and PM (adapted from (Sofiev et al., 2018))

Pollutant (Kt)	2012 estimate	2015 estimate	2020 estimate
SO_x	10,200	11,500	2500
PM	1400	1540	770

To predict the effects of the sulfur emission cap, one can investigate the outcomes of regulations already in place. By looking at the sulfur ECAs which have been in place since 2015 through MARPOL Annex VI, sulfur emission trends and their effects can be analysed. A study on the effectiveness of shipping ECAs in Shanghai, China, where most SO_x emissions were shipping-related, was carried out during 2015-17. Between two sample sites, SO_2 emissions reduced by 27% and 55%, despite shipping activity increasing by 7-10% during this time (Zhang et al., 2019). A reduction of 40% in sulfate aerosols was also observed. Interestingly, the emissions of V contained in particles increased from 1.4% to 6.9% which can be attributed to the increase in shipping activity and the continuation in the use of heavy fuel oils, with shipping companies opting to use EGCS instead of using low-sulfur fuels, (which also contain low concentrations of V).

One study on the Shanghai port area estimated a potential reduction of ~104,000 t SO_2 emissions per year through the successful implementation of its ECA in 2016 (Qin et al., 2017). Similarly, another study estimated that the implementation of an ECA covering the Baltic Sea

and the North Sea in 2010 would reduce annual SO_2 emissions by 23,000 t by 2030 (Campling, 2013). Extending the existing ECA in this area by 200 nm (370km) would result in a reduction of 160,000 t SO_2 emissions, while shipping related PM emissions were also predicted to be reduced by 66%.

Zetterdahl et al. (2016) carried out a sampling investigation on the effectiveness of a sulfur ECA in the Baltic Sea on the emissions of SO_x and PM implemented by MARPOL Annex Vi in 2015. The subsequent switching to 0.1% w/w sulfur fuels reduced PM and SO_x emissions by up to 67% and 80% respectively. In regions where ECAs are already in place, the change in atmospheric sulfur deposition will be slightly less noticeable, but still present to a high degree (Matthias et al., 2016). A reduction in sulfur emissions will depend on the change in shipping practices; in the case of changes in fuel type to ones with no sulfur content (such as LNG), reductions in SO_2 and SO_4^{2-} are predicted up to 80%. Meanwhile, in the case of installations of ECGS, reductions are predicted up to 60% (Matthias et al., 2016). The same study notes a visible reduction in shipping contribution to $PM_{2.5}$ concentrations.

1.15   Post-IMO-2020 strategies

High sulfur emissions are caused by the use of cheap marine high-sulfur heavy fuel oils (HS-HFOs). Daily global marine HFO consumption in 2018 stood at 3.38 million barrels with little to no use of low-sulfur fuel oils (Figure 1.3). Heavy fuel oils can be blended with distillates to produce intermediate fuel oils (IFOs). Alternatives to HFO to meet current SO_x limits are Light Sulfur Heavy Fuel Oil (LSHFO), Liquefied Natural Gas (LNG) and methanol mixed with fuel oils (Lindstad et al., 2017). Use of ECGS was observed in 2019 in preparation for IMO-2020 as well as the introduction of very-low or ultra-low sulfur fuel oil (ULSFO) with sulfur contents of below 0.1%. Low-sulfur alternatives to HFOs are generally expensive due to the cost of refinement. A combination of the use of HFOs and exhaust gas cleaning systems (EGCSs) has

proven to be most cost-effective while still remaining under the 0.5% sulfur (Lindstad et al., 2017). The move towards alternative fuels are seen in Figure 1.3, where the use of LSFO (low sulfur fuel oil) or scrubbed HFO was non-existent in 2018.
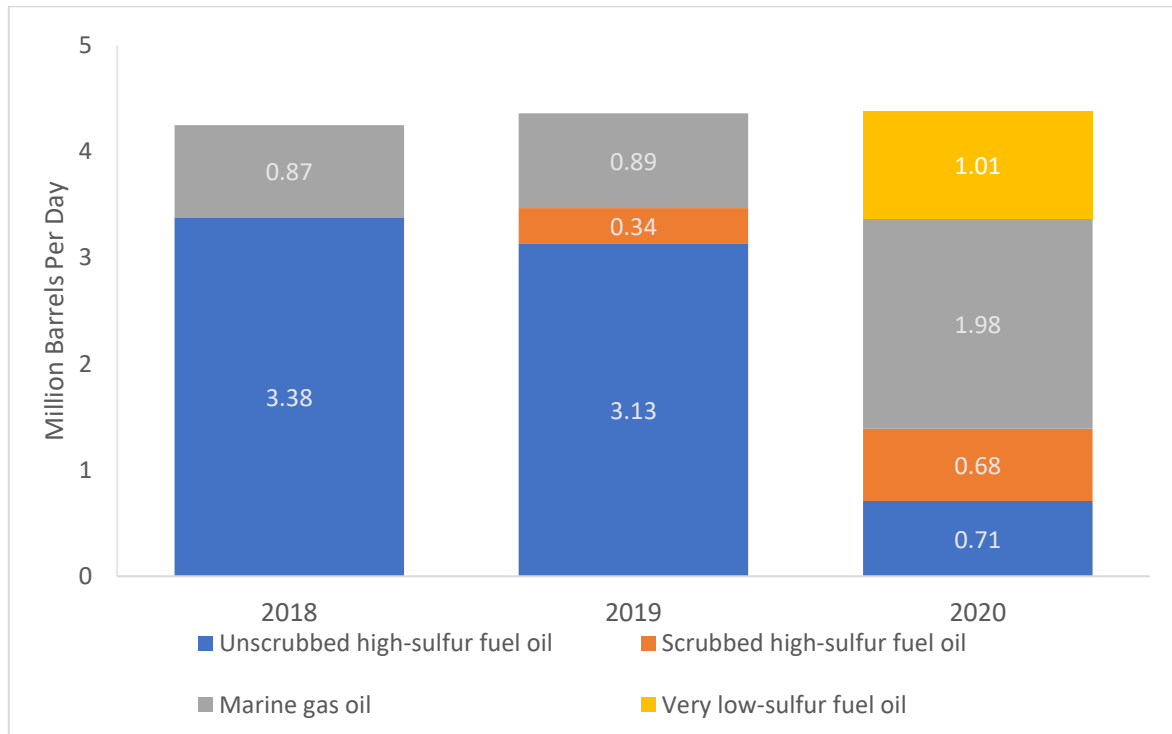
Figure 1.3 – Trends in daily consumption of different marine fuels, adapted from (Statista, 2021)

With the move towards ECGSs and the phase out of HFOs, there is great demand for alternative fuel sources (Deniz et al., 2016, Elgohary et al., 2015, Mohd Noor et al., 2018, Sergey et al., 2019, Wang et al., 2020). Aside from the already-used LNG and LSHFOs, biofuels, hydrogen, and methanol exist as energy sources, with the most suitable alternative currently being unclear (Platts, 2021). A comparison of fuel attributes is presented in Figure 1.4. Of those compared, marine diesel oil (MDO) is the only fuel containing sulfur, albeit at a negligible 350 ppm. Low carbon content is favourable due to the upcoming IMO 2030 and 2050 carbon emission regulations of a reduction of carbon emissions of 40% and 70% respectively (IMO, 2018). Methanol and ethanol are produced by the distillation of organic products, resulting in easily

produced fuels with relatively low carbon content and no sulfur content (Deniz et al., 2016). It must be noted that these fuels must be mixed with fuel oils and cannot be used as a marine fuel by itself. With lower density, higher volumes of fuels must be used, leading to a need for greater onboard fuel storage capacity, otherwise the total effective fuel capacity could be greatly reduced. In fact, in the case of LNG, the volume needed is double compared to the same effective volume of MDO (Elgohary et al., 2015).

Hydrogen is unique in having extremely low density and no carbon content. It is considered an extremely 'clean' renewable fuel, but with the drawbacks of requiring specialised containers and volumes of up to 7 times greater when compared to HFO (Deniz et al., 2016). As is the case with other alternative fuel sources, hydrogen is used in combination with other fuels. Biofuels such as ones derived from vegetable oil are also strong options due to high availability, but with the drawback of high production costs (Wang et al., 2020).
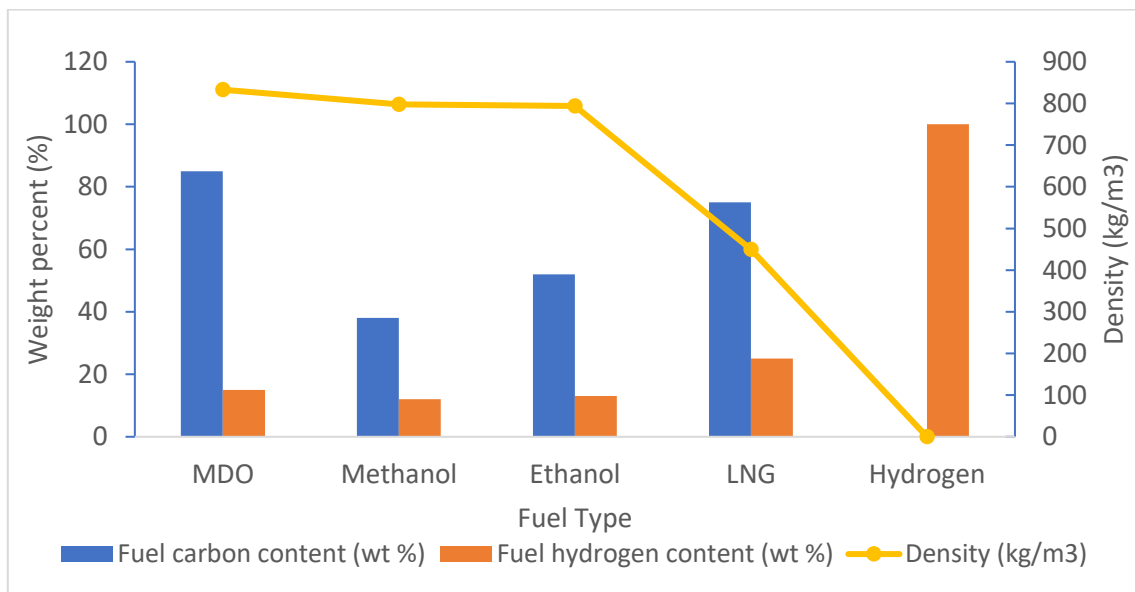
Figure 1.4. Alternative fuel types to classic marine fuel oils and their characteristics (Deniz et al., 2016)

It must be noted that with the implementation of new fuel types, each alternative comes with a variety of factors to be considered, such as production and storage costs, effects of engine performance, and changes in engine design to account for the new fuel. Ship owners must

decide on the most efficient alternative fuel while also considering current and future regulation changes.

Emission values for alternative fuels have been calculated by Gilbert et al. (2018), allowing for a strong comparison of new fuels (Figure 1.5). LHSFO (1% wt S) emits by far the highest concentrations of SO_x and PM, followed by MDO (0.1% wt S). The use of LHSFO post-2020 must entail installations of ECGS to reach the sulfur cap of 0.5% wt but would still be unusable in ECAs due to the 0.1% wt cap. Methanol, LNG and hydrogen produce little to no secondary pollutants, with hydrogen emitting no CO_2 by nature. Furthermore, we must consider the energy production potential of these fuels as an indication of the potential volume of each fuel needed. LSHFO, MDO, methanol, LNG and hydrogen have a net energy production of 40.5, 42.6, 48.6, 120 and 20 MJ/kg respectively. CO_2 levels for all fuels bar hydrogen are relatively high.

Alternative fuels have great potential, particularly in achieving IMO-2020 regulations. However, as we look towards the future, CO_2 emission values for the majority of fuels reviewed are problematic when considering upcoming regulations (IMO-2030 and IMO-2050). Hydrogen stands out as the 'cleanest' fuel option, but is currently weighed down by production cost, in particular the need for further hydrogen-fired power stations (Atilhan et al., 2021)
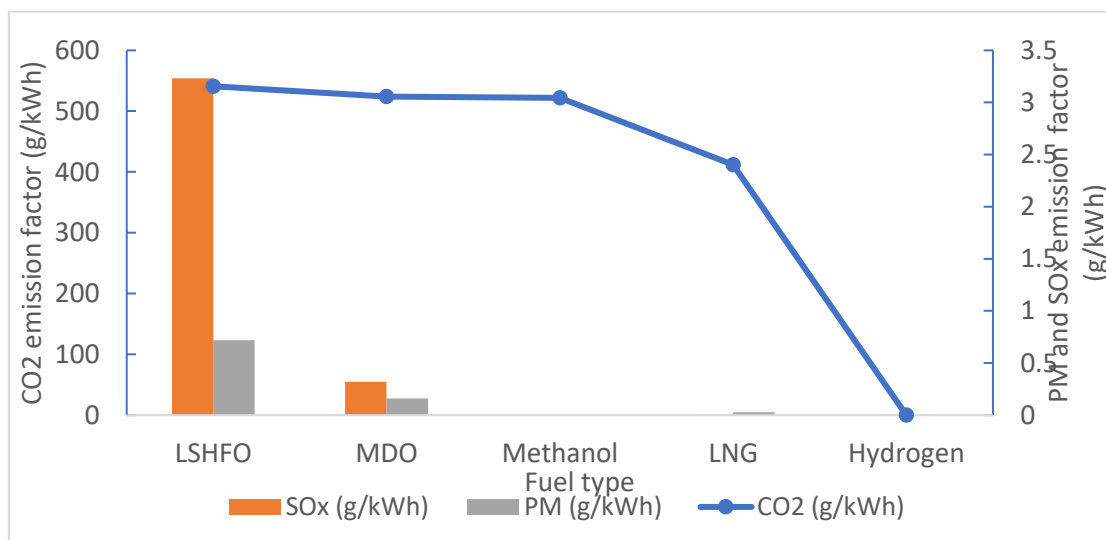
Figure 1.5. Emission factors for different marine fuel types (Gilbert et al., 2018)

1.16   Research Aims and Objectives

The project aims to investigate temporal changes to aerosol chemical character following changes to shipping regulations using new and archived aerosol samples from Western English Channel (WEC).

The key objectives for this work can be summarised as:

1. Complete a literature review on:

    a. Atmospheric trace elements in the marine environment

    b. Shipping emissions, their quantification and their environmental effects

    c. IMO-2020 regulations, strategies and predicted effects

2. Process and analyse aerosol samples from a coastal atmospheric observatory (Penlee Point Atmospheric Observatory) in southwest England by performing leaches and digests on aerosol loaded filter samples and analysis of these using IC and ICP methods.

3. Quantification of nss-SO_4^{2-}, major ions, trace metals and other markers of atmospheric shipping emissions to the atmosphere and ocean surface from the Western English Channel (WEC).

4. Identify aerosol sources using meteorological data and chemical characteristics (e.g. elemental ratios) of contrasting aerosol populations.

5. Interpretation of data to elucidate environmental significance and assess influence of the IMO-2020 regulation.

6. Investigate the use of the V/Ni ratio as a marker of shipping emissions.

Chapter 2. Materials and Methods

2.1 Sample Site

Penlee Point Atmospheric Observatory (PPAO; $50°19.08'$ N, $4°11.35'$ W, see Figure 2.1 & 2.2) is a coastal observatory on the southwest coast of England. The observatory is situated at 11 m above sea level and is considered a suitable site to study marine atmospheric chemistry, with extensive research being done on air-sea exchange, sea salt fluxes and shipping emissions (Thomas et al., 2016, Yang et al., 2016, Yang et al., 2019). It is ideally located to pick up Atlantic air masses from the southwest and air masses from the southeast contaminated by shipping exhaust fumes and European continental airmasses, and should theoretically be sensitive to any changes, such as those after the introduction of IMO-2020. Continuous measurements of CO_2, CH_4, O_3 and SO_2 have been recorded at the site, as well as meteorological variables including temperature, humidity and pressure, since its development in 2014.

Two previous datasets will be used to compare trace element and major ion atmospheric concentrations pre- and post-IMO-2020. Trace element results post-IMO-2020 will be compared to a previous dataset taken from PPAO. The study by postgraduate student Sov Atkinson (University of Plymouth) ran from January 2015 to August 2016. Major ion results will be compared to results from the February 2017 to September 2018 study by postgraduate student Caroline White (University of Plymouth).

Figure 2.1. PPAO sample site

Figure 2.2. Geographical location of PPAO (Google Maps,

https://goo.gl/maps/g1mXBmRUTsG37VmS8, retrieved August 12, 2022)

2.2 Sampling Protocol

The sampling was conducted as part of the Atmospheric Composition and Radiative forcing changes due to UN International Ship Emissions regulations project (ACRUISE, NERC Highlight Topic, PI Ming-Xi Yang, PML). The project aims were to investigate the effect of the IMO-2020 regulation on atmospheric chemistry and climate using multiple scientific

observations. For the sampling in this study, 8" x 10" filter sheets (Whatman 41, cellulose) and slotted cascade impactor sheets (Tisch, cellulose) were used as collection substrates, rinsed and dried before loading onto the filter holders. Aerosol size fractionation was used to sample both the coarse and fine fractions, classed as (ca. >1 µm) and (<1 µm) respectively, using a single stage cascade impactor with nominal cut off size of 1 micron (Tisch).

A 24-hour sample time was aimed for and the pump was turned on remotely at an average flow rate of 39.8 m^3/h when consistent wind directions were detected from the South (air masses crossing the English Channel shipping lane). Otherwise, a 24 h period would be turned on manually, to achieve a minimum of one sample per week. Samples were collected from the site weekly and removed from filter holders with acid-washed plastic tweezers. Filter samples were stored in plastic zip-lock freezer bags, kept frozen at -20 ºC ready for analysis. Sample filters for analysis were cut with a 19 mm arch punch (punch sanded and polished with ethanol and water) for the 8 x 10" sheets, or strips cut directly from the cascade impactor sheet. Three arch punches had a combined surface area of 0.11 cm^2 whereas the cascade impactor strip had a surface area of 5.25 cm^2.

The pre-2020 sampling for major ions and nutrients (2017-18) was similar to that of the current project, aside from two important points: (i) all the values reported for pre-2020 are 'total' aerosol (combined values for fine and coarse fractions) due to the lack of a cascade impactor to separate the two fractions, (ii) for all pre-IMO-2020 samples, the 24 h pump activation condition of identifying a consistent wind direction for a 24 h period during each week, whereas consistent wind direction from the south (ocean) was used in the current project (Post-2020). Trace metal sampling pre-IMO-2020 was performed by Sov Atkinson (2015-2016, University of Plymouth) who used a low-volume aerosol sampler which was run at PPAO at an average rate of 39.8 m^3/h. A key point is that aerosol samples were collected at the same site using low-volume samples (as opposed to the high volume 8 x 10" filters used in this study). Acid-washed

Mixed Cellulose Ester (MCE) membrane filters were mounted onto Savillex PFA filter holders. These were housed in a plastic weather shield with a 4.5 cm diameter opening underneath. A rotary vain pump (GAST, UK) was turned on/off when a constant wind direction was forecasted for 24 h.

2.3 Trace Metal Analysis (ICP-MS)

Analysis was carried out at a University of Plymouth laboratory. Due to the analysis of trace metals, appropriate measures were carried out to prevent contamination of samples. Polyvinylchloride gloves and sleeves were worn for all sample and equipment handling and were changed repeatedly. Sampling was carried out in a laminar flow cupboard (Bassaire, <100 particles of size >0.5 µm per ft^3), regularly wet damped or rinsed with high purity water and dried to avoid the build-up of dust particles. Equipment and glassware were acid-washed overnight in 10% v/v HCl (Fischer Scientific, 37% analysis grade) to remove metal and organic contamination. An ultra-pure water system (Millipore, UK) was used to obtain >18 MΩ cm ultra-pure water (UPW). Acid-washed equipment was rinsed using UPW and carried out 5 times per item. When necessary, acid-washed glassware was stored in 0.01M HCl (Fischer Scientific, 37% analysis grade). Filter sheets and leached samples were stored in a freezer at -20°C.

To obtain a water-soluble fraction, 50 ml sonicated water leachates were filtered through a Savillex filtration system (QMX laboratories, UK, see Figure 2.3) connected to a vacuum pump. Polycarbonate filters (Whatmann, 47 mm, 0.45 µm) were prepared by soaking in 0.5 M HCl and rinsing 5 times with UPW. Sample filters were placed in 50 ml UPW for 30 seconds before being filtered and passed through the 47 mm filter into the collection chamber. The filtration system was rinsed 5 times between each sample. 15 ml of each sample was stored in plastic centrifuge tubes, spiked to 2% HNO_3 (Romil, UpA grade) for one week to dissolve

metal species with 25 ppb In/Ir as an internal standard for ICP-MS. The process was repeated for cascade impactor sample strips. Leachates were analysed using an iCAP^{TM} RQ ICP-MS (Thermo Fisher Scientific, UK). Trace metal processing analysis for the pre-IMO-2020 project was carried out in the same way, with the small exception of using gravity to leach through the filter instead of a vacuum pump.

The accuracy of the analysis was tested using a certified reference material (CRM, EnviroMAT drinking water EP-L) at a 1000-fold dilution to calculate instrument bias, as well as analytical/procedural blanks and a repeated measurement check standard, run between samples using an autosampler.

Elements chosen for analysis were Be, Al, Si, P, V, Cr, Mn, Fe, Co, Ni, Cu, Zn, As, Cd, Sb and Pb.

Figure 2.3. Savillex 47mm filter holder

2.4 <u>Major Ion Analysis (Ion Chromatography)</u>

Three punches of sample filters were placed in plastic centrifuge tubes in 15 ml UPW and sonicated for 1 h to allow for the water-soluble fraction of aerosols on the filters to leach. Samples were then refrigerated for 23h at -4ºC, ready for subsequent IC analyses. Technical details and settings on the IC system are seen in Tables 2.1 and 2.2.

Table 2.1. Anion and Cation IC column specifications

	Guard Column	Analytical Column	Suppressor	Eluent	Heater Temp	Flow rate	Elution
Anion	2 mm AG-23	2mm AS-23	AERS 500	4.5 mM Na_2CO_3	30 ºC	0.25 ml/min	Isocratic
Cation	3 mm CG-12A	3mm CS-12A	No suppressor	20 mM MSA	30 ºC	0.5 ml/min	Isocratic

Calibration standards were prepared by mixing salts (>95% reagent grade) and ultrapure water. Salts were desiccated in an oven at 40℃ for 1 h before measuring on a balance. After weighing, solutions were mixed using a shaker table. 1M HCl (Fischer Scientific, 37% analysis grade) was used to aid dissolving in the cation solution. Two calibration standards were made. Anion solution contained NaCl, $NaNO_3$, NaBr, KH_2PO_4 and Na_2SO_4. Cation solution contained NaCl, NH_4Cl, KH_2PO_4, $MgCl_2$, $CaCl_2$ and HCl. Solutions were mixed with UPW and stored in 5 L acid cleaned volumetric flasks. Calibration concentrations were calculated and respective dilutions were carried out.

Tables 2.2 and 2.3. Cation (left) and anion (right) calibration standard constituents and

concentrations in 5 L stock standard

Cation	Concentration (mg L^{-1})
Na$^+$	200
NH$_4^+$	250
K$^+$	500
Mg^{2+}	250
Ca^{2+}	250

Anion	Concentration (mg L^{-1})
Cl$^-$	30
NO$_2^-$	100
Br$^-$	100
NO$_3^-$	100
PO$_4^{3-}$	150
SO$_4^{2-}$	150

IC sample runs consisted of calibration standards, check standards, analytical and procedural blanks, and samples, run in triplicate injections. Chromeleon^{TM} version 7.2 software was used to analyse chromatographs and calibrate the equipment. The Cobra wizard tool was used to process chromatographs and smart peaks to integrate and detect peaks using industry standard algorithms.

2.5 Data Conversions

ICP-MS and IC results were converted from leach sample concentrations (μg L^{-1}) to concentrations in air (ng/m^3 and pmol/m^3). Order of conversions are represented in Figures 2.4 and 2.5.

Blank subtraction   * Leach volume 9 ml   * Ratio punches to sheet

| Total leach concentration in 9 ml ($\mu g\ L^{-1}$) | Total leach concentration in 9 ml sample without blank | Total element mass in 9 ml (μg) | Total element in filter sheet from 9 ml (μg) |

Conversion to pmol/m3   /Total volume air   * Ratio 50/9

| Total elemental concentration in air (pmol/m^3) | Total elemental concentration in air (μg/m^3) | Total element in filter sheet from 50 ml (μg) |

Figure 2.4. Data conversions for ICP-MS trace element data

* Ratio punches or cascade strip to filter sheet

Blank subtraction   * Leach volume 15ml

| Total leach concentration in 15 ml ($\mu g\ L^{-1}$) | Total leach concentration in 15 ml sample without blank | Total ion mass in 15 ml leach (mg) | Total ion mass in filter sheet from 15 ml (μg) |

Conversion to pmol/m3   /Total volume air

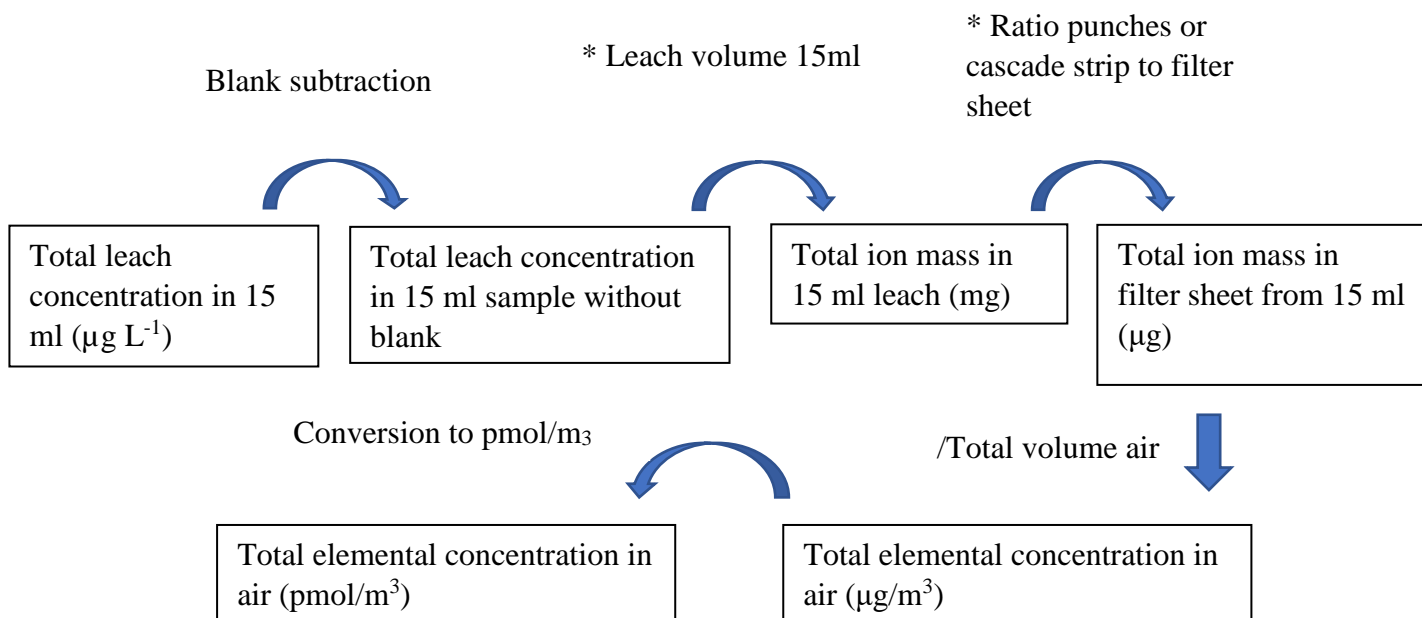| Total elemental concentration in air (pmol/m^3) | Total elemental concentration in air (μg/m^3) |

Figure 2.5. Data conversions for IC major ion data

2.6 <u>Back trajectory Analyses</u>

The HYSPLIT model was created by the National Oceanic and Atmospheric Administration (NOAA) and Australian Bureau of Meteorology Research Centre (ABMRC) in 1998. The model uses data from the Global Data Assimilation System (GDAS). It is widely used to track air masses, with numerous uses in researching forest fires, dust events and airborne pollutants (Stein et al., 2015). It has allowed for a greater understanding of the transboundary transport of aerosols, especially useful when interpreting aerosol data; back trajectories can help decide whether pollution at a sampling point was affected by local sources or carried by wind from a farther source.

The web-based HYSPLIT model was run from the Real-Time Environmental Applications and Display System (READY) site, using GDAS 1-degree data. A back trajectory was run at the ending time of each sample to create back trajectories per sample air mass. The HYSPLIT model was run at 50, 500 and 1000 m above sea level for a total of 120 h. A map detailing sector areas around PPAO created by White et al., based on an analysis of local wind directions at the observatory, is seen in Figure 2.6 (White et al., 2021, Yang et al., 2016). The sectors define air mass sources regions which, in conjunction with Back trajectory models, can be used to classify sample air mass sources. The 50m back trajectory height was used. Back trajectory example runs are seen in the appendix (Figures A1-4).

Air mass sector classification was decided based on total hours spent in each sector within the 120 h period. However, air masses that crossed over areas with high anthropogenic activity were considered and discussed individually. This weighting was done for 'clean' Atlantic air masses that crossed over or near sectors containing high anthropogenic activity, whose air mass was classified based on the last 24 h period. The weighting helps to prevent skewed Atlantic masses with high concentrations of anthropogenic-sourced air masses, which are typically not

45

found in air masses passing over the Atlantic. A breakdown of sample numbers per air mass are found in Table 2.4.
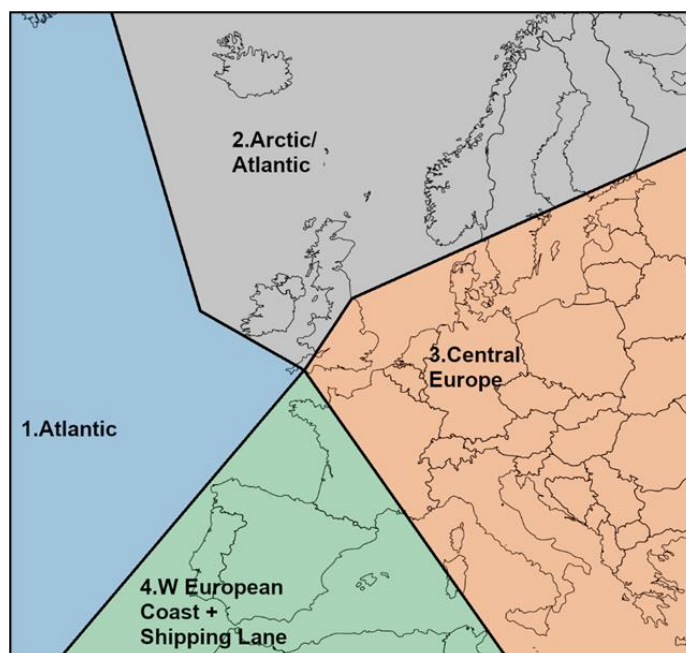
Figure 2.6. Air mass sector classifications developed by (White et al., 2021)

Table 2.4. Sample number breakdown by season and sector across all datasets. Sector data unavailable for the trace metal Pre-IMO-2022 dataset.

	Number of samples	Pre-IMO (2015-16)	Pre-IMO (2017-18)	Post-IMO (2019-20)
Season	Spring	13	21	21
	Summer	18	16	14
	Autumn	9	10	8
	Winter	11	9	10
Sector	Mainland UK/Ireland		21	11
	Central Europe	N/A	11	9
	Unregulated Shipping		8	21
	Clean Marine		16	12
Total		51	56	53

2.6.1 Clean Marine

The Clean Marine sector represents a region with 'clean' Atlantic air masses largely unaffected by anthropogenic activity except for the long-range transport of aerosols from North America, and some marine vessels crossing the Atlantic. Mostly, however, the sector has considerably low marine activity, and, as such, is relatively unaffected by shipping emissions.

2.6.2 Mainland UK/Ireland

The Mainland UK/Ireland sector contains mixed air masses containing inland emissions from the UK, Ireland, and Scandinavia as well as Atlantic air, including shipping emissions from vessels navigating these waters. The sector includes a small section of the North Sea SECA, in which vessels navigating the area must use 0.1% S m/m fuels, as stated in MARPOL Annex VI (IMO, 2005).

2.6.3 Central Europe

The Central Europe sector contains South-East England and the majority of Central Europe, an area rich in industrial activity, as well as a large section of the English Channel, whose shipping lanes have high levels of marine traffic all year round. All vessels in the sector are navigating the SECA.

2.6.4 Unregulated Shipping

The sector covers Spain, Portugal and South-West France, which are also being affected by plumes emitted in the shipping lane. Sector classifications for air masses allows for an understanding of their sources, providing a deeper analysis of samples. A section of the waters in this sector includes the SECA, however, it is assumed the majority of vessels are navigating under standard international fuel regulations, i.e. 3.5% w/w S and 0.5% w/w S fuels pre- and post-IMO-2020 respectively.

2.7 Blanks, Limits of Detection and Accuracy

Procedural blank filters were prepared using the same methodology as samples but placed on the sampler without the pump on for 5 minutes (n=10). The limits of detection for both analyses were calculated using 3 * standard deviation of procedural blanks (see Tables 2.5, 2.6 and 2.7). Blank subtractions were carried out using mean across all procedural blanks. Relative standard deviation for ICP-MS was calculated using 3 repeated-measurement check standards (4, 10 and 20 µg L^{-1}) (see Table 2.7). A check standard example for V is seen in Figure 2.7. Average standard deviation of the 3 check standards was calculated, with the relative standard deviation being calculated with the equation (1)

$$RSD = \frac{mean\ \sigma}{mean\ check\ standards} \times 100\% \tag{1}$$

Relative standard deviation was used to calculate error for each sample. CRM sampled value was then divided by the original CRM value used to calculate error percentage. The CRM did not include Si. Major ion relative standard deviations were calculated using the same method using triplicate injections.

The results from the CRM for this study can be found in Figure A5 in appendix. Analysis of Si and Ag produced no value, therefore an unknown agreement with the CRM. Differences of over 20% were found for Al, P, Cd, Sb and Pb so this level of uncertainty should be considered when interpreting the results for these elements. Strong agreement with the CRM was found for V and Ni (5.9% and 3.1%, respectively), providing greater quality assurance for the two most important elements.

Table 2.5. (left) Procedural blank filter analysis results for ICP-MS (showing mean check standard standard deviations, relative standard deviation and % error from the certified reference material) and Table 2.6. (right) check standards standard deviations for IC analysis.

Element	Mean Chk Std StDs	RSD	CRM Error (%)
Al	0.59	0.03	48.98
Si	7.32	0.08	N/A
P	1.32	0.06	21.56
V	0.21	0.02	5.90
Cr	0.18	0.02	7.72
Mn	0.20	0.02	11.21
Fe	0.50	0.03	4.90
Co	0.19	0.02	2.12
Ni	0.21	0.02	3.11
Cu	0.20	0.02	0.68
Zn	0.24	0.02	12.93
As	0.18	0.02	9.94
Cd	0.07	0.01	27.46
Sb	0.08	0.01	24.73
Pb	0.13	0.01	38.45

	Procedural blank filter	
Ion	Mean (μg L-1)	StD (μg L-1)
F^-	<LoD	<LoD
Cl^-	0.44	0.17
NO^{2-}	<LoD	<LoD
Br^-	<LoD	<LoD
NO^{3-}	<LoD	<LoD
SO_4^{2-}	0.36	0.07
PO_4^{3-}	<LoD	<LoD
Na^+	0.33	0.16
NH^{4+}	0.15	0.11
K^+	0.05	0.02
Mg^{2+}	0.02	<LoD
Ca^{2+}	0.04	<LoD

Table 2.7. Blank filter analysis for IC analysis

	Procedural blank filter		
Element	Mean	StD	LOD (3*SD)
Al	1.778	0.419	1.258
Si	82.832	9.608	28.824
P	6.829	0.865	2.595
V	0.0023	0.0007	0.0022
Cr	0.065	0.014	0.042
Mn	0.013	0.004	0.011
Fe	0.425	0.092	0.277
Co	0.0012	0.0004	0.0012
Ni	0.050	0.013	0.040
Cu	0.026	0.009	0.026
Zn	0.557	0.300	0.900
As	0.011	0.003	0.010
Cd	0.004	0.002	0.007
Sb	0.004	0.002	0.006
Pb	0.038	0.048	0.143
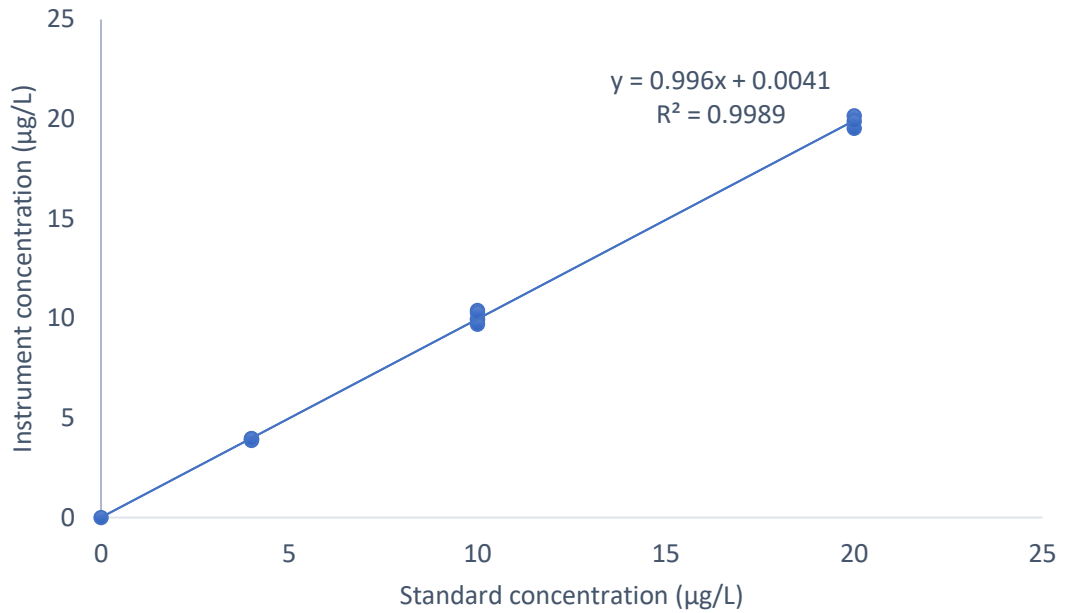
Figure 2.7. Repeated check standard example for V

2.8 Data handling and Quality Control

Data was flagged under certain conditions with action being taken to treat these cases (Table 2.8)

Table 2.8. Flagging data and actions.

Reason for flagging	Subsequent action
Missing fine/coarse fraction data	Kept in analysis
Negative values (ICP-MS)	Replaced with calculated LoD
<Limit of detection	Kept in analysis
Missing triplicate injection results (IC)	High or no uncertainty values (in the case of just 1 injection result) – kept in analysis
Negative nss-SO_4^{2-} (IC)	In samples where the respective uncertainties could not cross into positive values, omitted from analysis. Otherwise, set to zero.

2.9 Statistical Analysis

Microsoft Excel^{TM} 2019 software with the Analysis ToolPak extension and IBM® SPSS® Statistics were used to carry out data analysis. Descriptive statistics were calculated for each element in the dataset. Unless stated otherwise, medians were used for analytical discussions including comparisons with previous datasets and other research papers.

2.9.1 Spearman's Correlation

The Spearman's rank correlation coefficient test was run using the Microsoft Excel Analysis ToolPak add-on to test correlations between variables at the 0.05 confidence level. The method tests for significant correlations for a non-parametric dataset,

$$\rho = 1 - \frac{6 \sum d_i^2}{n(n^2 - 1)} \qquad (2)$$

Where d_i is the difference in ranks and n is the number of observations.

Correlations were run between elements as a method of source appointment. Significant correlations between elements often emitted by ships, such as V, Ni and Sb, could indicate ship emissions. Similarly, in elements commonly found in the upper continental crust, correlations could indicate dust events. Elemental correlations were also run for each season, to investigate fluctuations in emissions with seasonality, as well as sector correlations being analysed to investigate common sources of emissions in each sector.

2.9.2 Mann-Whitney U

The Mann-Whitney U test was determined using SPSS software to find significant difference between groups and non-normal datasets, at the 0.05 confidence level. The test was run between elements in different seasons, to locate variability in element emissions with seasonality. The test was also run to compare the 2019-21 dataset with the previous pre-IMO-

2020 dataset, in order to observe changes in atmospheric concentrations over time, allowing for a discussion on the efficacy of the IMO-2020 regulation. 10 common elements were analysed between the datasets. Similarly, statistical differences in V/Ni ratios between the two datasets were investigated, due to the likely changes in the emissions of these two elements with new shipping practices. Significant difference was also tested on elements between sectors to give an insight into differences in aerosol character within the regions analysed.

2.9.3 Charts

Box and Whisker diagrams and bar charts were created using Excel software and MATLAB^{TM} (2022), allowing for a visual interpretation of variability in elements over seasons and sectors, as well as comparing to the pre-IMO-2020 dataset. Excel software was also used to produce calibration charts. Stacked histograms were created using SPSS to visualise distributions of elements in both datasets.

Chapter 3. Results and Discussion

The aim of the work presented in this chapter is to assess the impact of the IMO-2020 regulation on marine aerosols through comparisons of pre- and post- regulation atmospheric datasets from the Penlee Point Atmospheric Observatory (PPAO). The results from the analysis of new samples from 07/2019 to 06/2021 (termed 'post IMO-2020') and any other supporting data will be presented. These current observations of atmospheric trace element and major ion concentrations will be compared to currently unpublished supporting data from previously collected samples from the same atmospheric station. The dataset by Sov Atkinson (University of Plymouth) from January 2015 to August 2016 analysing atmospheric trace elements, and a dataset from Caroline White (University of Plymouth) analysing major ions between February 2017 to September 2018 will be termed 'pre-IMO-2020'. The focus is on identifying the effect of the IMO-2020 regulation and identifying any significant changes in aerosol chemistry relating to these changes. Specifically, this chapter:

1. *Investigates changes in the aerosol V/Ni ratio and evaluate the viability of using the ratio as a marker of shipping emissions*

2. *Compares temporal seasonal changes and air mass characterised atmospheric trace element and major ion concentrations around PPAO*

3. *Investigates correlations between trace elements of interest*

4. *Calculates* nss-SO_4^{2-} *post-IMO-2020 and determine changes in concentrations in comparison to pre-IMO-2020*

3.1.1 Aerosol trace element results

Following the analysis of aerosol filter samples by ICP-MS, atmospheric trace metal concentrations were compared pre- and post-regulation. Water-soluble V and Ni concentrations and their subsequent ratios are presented, referring to similar literature on the change of these elements after the implementation of shipping regulations. Data from the two previous datasets will not be described in detail and used solely to compare current results.

A total of 64 aerosol filter samples were usable for the analysis of trace elements. As detailed in Chapter 2, these samples were taken from PPAO as a representation of the composition of different aerosols passing the sample site. Seven samples were taken in 2019, 38 in 2020 and 19 in 2021. Samples taken from July to December 2019 will be considered as post-IMO-2020 samples, under the assumption that IMO-2020 measures were introduced before the 1st January 2020 cut-off date.

As previously stated, the use of medians for comparison was prioritised and used instead of mean averages due to the non-parametric nature of aerosol data. Figure 3.1 below shows the log-normal spread of the elemental analyses on a log scale for the post-IMO-2020 samples. Lighter metals such as Al and Zn are found in higher concentrations than other elements due to their abundance in the atmosphere, as well as those metals found in the Earth's crust (Taylor et al., 1995).

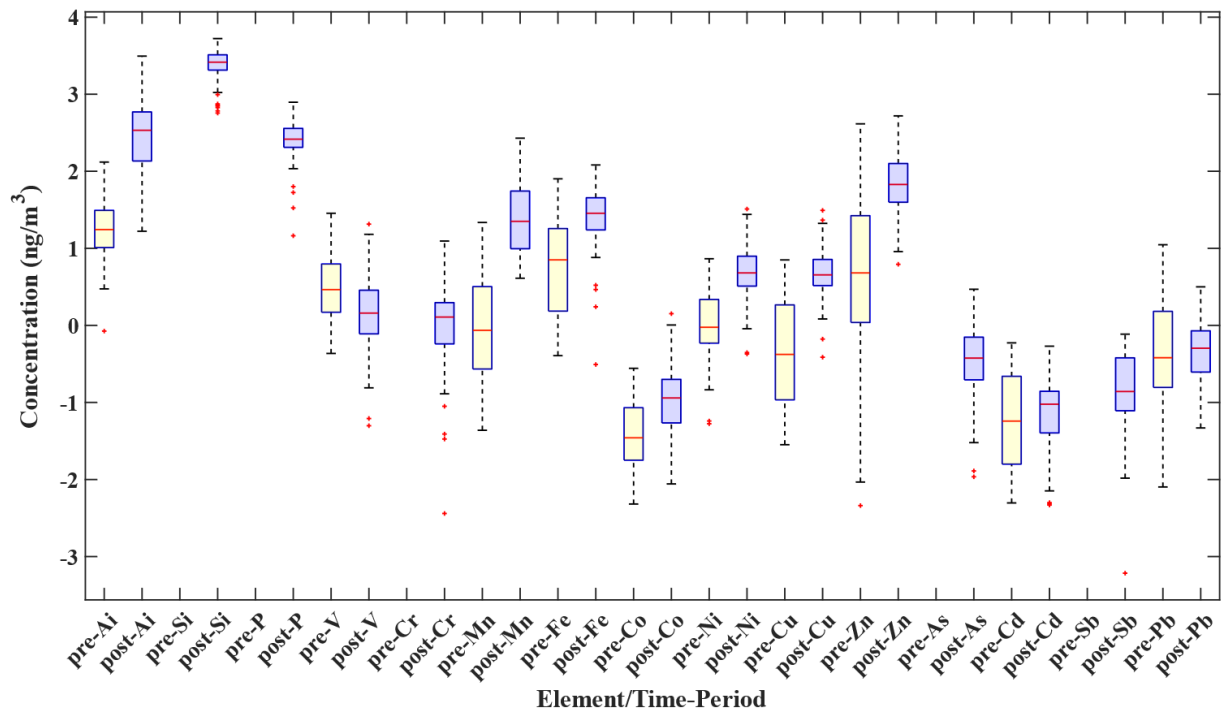Figure 3.1. Box and whisker diagram for pre- and post-IMO-2020 atmospheric trace element concentrations around PPAO. Some elements were not analysed for the pre-IMO-2020 dataset and are thus not shown.

3.1.2 <u>Descriptive post-IMO-2020 trace element data</u>

Descriptive data for atmospheric elemental concentrations are presented in Table 3.1 While other elements are mentioned, the focus of this section is on V and Ni.

Table 3.1 - Descriptive statistics for pre- and post-IMO-2020 air concentrations from elemental ICP-MS analysis. Elements with significant difference between datasets are in bold (p<0.05).

Values in pmol/m³		Al	V	Mn	Fe	Co	Ni	Cu	Zn	Cd	Pb	Si	P	Cr	As	Sb
Post-IMO	Mean	515.2	2.87	40.66	37.09	0.211	7.24	6.47	96.62	0.107	0.67	2544	287	1.871	0.56	0.242
	Median	**340.2**	**1.44**	**22.40**	**28.49**	**0.114**	**4.80**	**4.52**	**67.31**	0.095	0.51	2602	261	1.284	0.38	0.139
	Minimum	16.66	0.05	4.09	0.31	0.009	0.43	0.39	6.21	0.005	0.05	569	15	0.004	0.01	0.001
	Maximum	3121.4	20.62	268.89	120.78	1.419	32.37	31.08	523.15	0.537	3.16	5274	787	12.439	2.94	0.769
	Count	62	63	61	57	59	53	63	63	63	64	61	63	52	62	63
Pre-IMO	Mean	26.04	4.88	2.56	13.51	0.058	1.60	1.06	24.70	0.129	1.37					
	Median	**17.53**	**2.91**	**0.86**	**7.08**	**0.035**	**0.95**	**0.42**	**4.79**	0.057	0.38					
	Minimum	0.84	0.43	0.04	0.40	0.005	0.05	0.03	0.00	0.005	0.01					
	Maximum	131.65	28.51	21.65	79.77	0.277	7.33	7.07	412.64	0.593	11.13					
	Count	51	51	51	51	51	51	51	49	51	51					

3.1.3 Do atmospheric trace elements post-IMO-2020 fluctuate based on season?

Figures 3.2 and 3.3 display V and Ni seasonal distributions, respectively. Post-IMO-2020 results for V ranged from 0.05 to 21 pmol/m^3 (mean 2.9 pmol/m^3, median 1.4 pmol/m^3). Highest values were found during summer (1.9 pmol/m^3) and the lowest for winter (0.9 pmol/m^3). Winter concentrations were significantly lower than in spring and summer ($p<0.05$), whereas no variation was observed during the other seasons. Ni results post-IMO-2020 ranged from 0.4 to 32 pmol/m^3 (mean 7.2 pmol/m^3, median 4.8 pmol/m^3). The highest values were found during winter (7.2 pmol/m^3) and lowest during autumn (4.2 pmol/m^3). Winter values were found to be significantly greater than the other seasons ($p<0.05$) with the latter showing no variation.
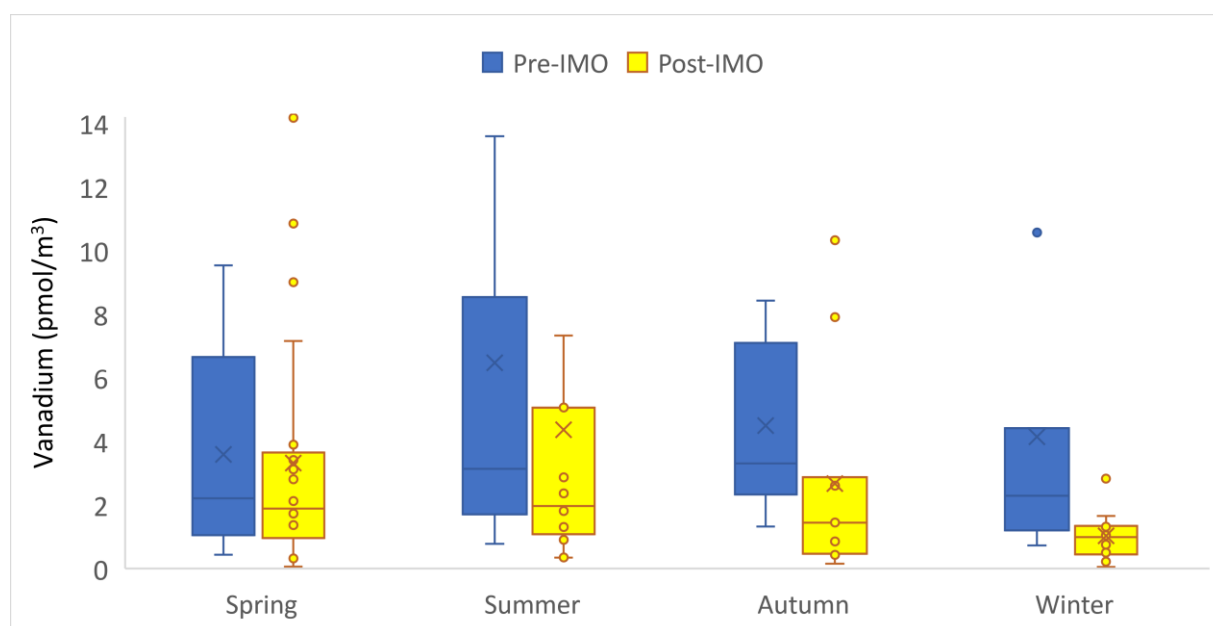

Figure 3.2. Seasonal distribution of vanadium pre- and post-IMO-2020. Some outliers not visible.
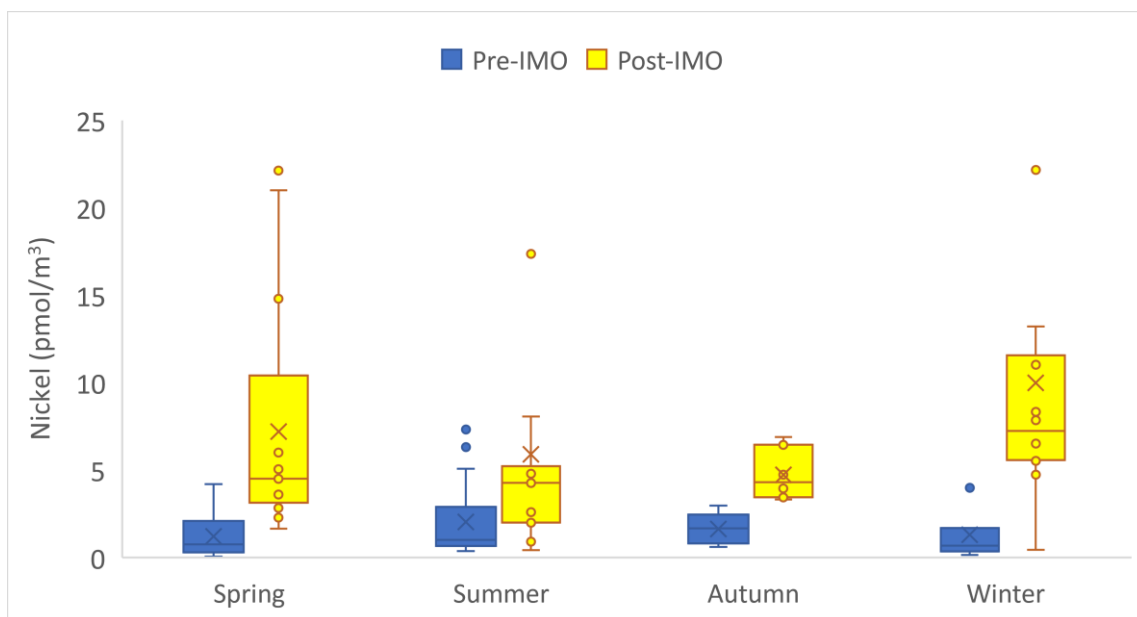
Figure 3.3. Seasonal distribution of nickel pre- and post-IMO-2020.

3.1.4 How do atmospheric trace elements post-IMO-2020 differ based on air mass classification?

Investigating air masses and the chemical character of their respective aerosols provides a stronger interpretation for elements used as shipping emission markers. As air masses can show great variation depending on wind speed, direction, aerosol emission sources and time spent traversing over different regions, classifying air masses can be complex. Aerosol elemental results were separated by the aforementioned air mass classifications (see Methods section 2.6). Focusing on V & Ni, Figures 3.4 and 3.5 display the distribution of V and Ni concentrations within each air mass.

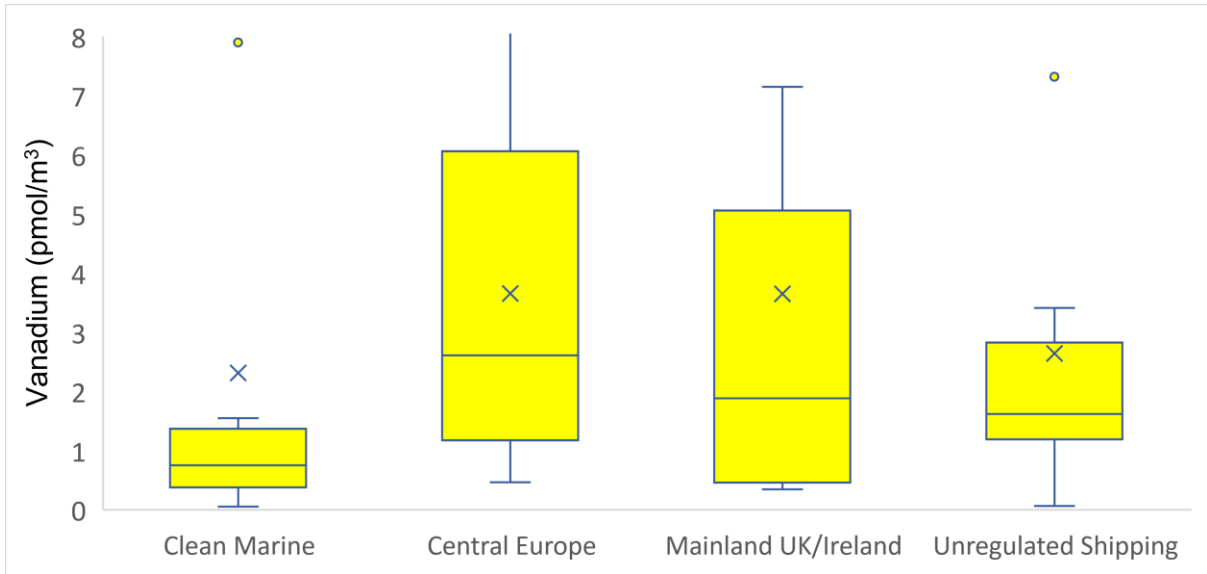Figure 3.4. Vanadium distribution over air mass classifications post-IMO-2020. Air mass classifications derived from time spent in respective sectors using backtrajectories. Upper whisker of Central Europe class not visible in order to scale axis (value 11 pmol/m^3).
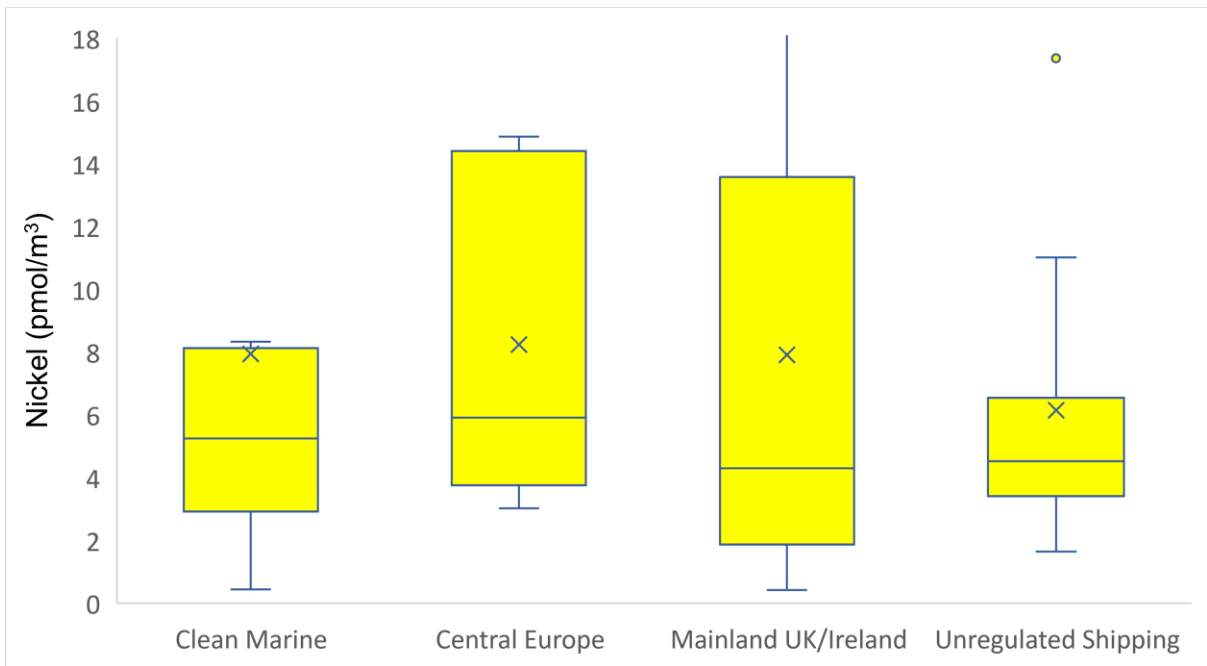

Figure 3.5. Nickel distribution over air mass classifications post-IMO-2020. Upper whisker not visible in order to scale axis (28 pmol/m^3).

Clean Marine

Detectable Ni was found in the Clean Marine air mass classification, while the lowest V concentrations were found in this sector (5.3 and 0.8 pmol/m^3 respectively, see Figure 3.4). However, the range of data in this sector was large, indicating possible anthropogenic emission sources influencing the air mass. High Ni concentrations could be attributed to global-scale long range transport of fine aerosol (fly ash) industrial activity, presumably from northern US states and southern Canada in cases where air masses passed over these areas within a 120-hour period. Emissions from the combustion of oils and fuels over land could account for elevated elemental concentrations since the impact of shipping activity over the Atlantic on the sector's air masses is negligible.

Mainland UK/Ireland

While the Mainland UK/Ireland air mass contained air masses passing mostly through the Atlantic, most passed over or around the British Isles and are thus influenced by both marine and terrestrial emissions of anthropogenic origin. Mainland UK/Ireland V levels were significantly higher than the Clean Marine air mass ($p < 0.05$), possibly indicating the presence of ship or land derived emissions (Figure 3.4). Ni values were not significantly different compared to the other air masses; however, it showed a large spread of datapoints, indicating a wide range of emission sources aside from shipping activity.

Central Europe

V and Ni datapoints lay in a wide range in the Central Europe air mass, indicating multiple emission sources. Central Europe V and Sb levels were significantly greater than those in the Clean Marine air mass ($p < 0.05$), which can be attributed to greater and more concentrated marine activity within the air mass.

<u>Unregulated Shipping</u>

Significantly greater V concentrations were observed over the Clean Marine air mass ($p < 0.05$). Aside from this difference, V and Ni concentrations in the Unregulated Shipping sector were not significantly different to the other air masses but, showed a lower range. The close spread of data indicates a smaller variety of emission sources, most of which are likely from shipping activity.

3.1.5 <u>How have trace element concentrations changed due to IMO-2020 regulation</u>*?*

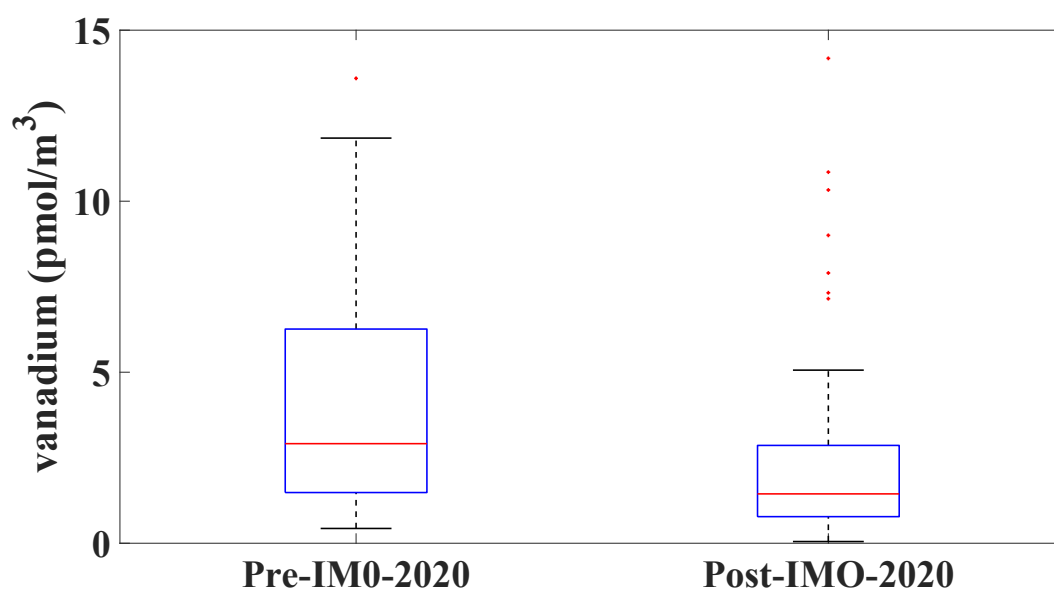Changes in V and Ni concentrations can be seen in Figure 3.6 and 3.7.

Figure 3.6. Comparison of vanadium concentrations pre- and post-IMO-2020 around PPAO
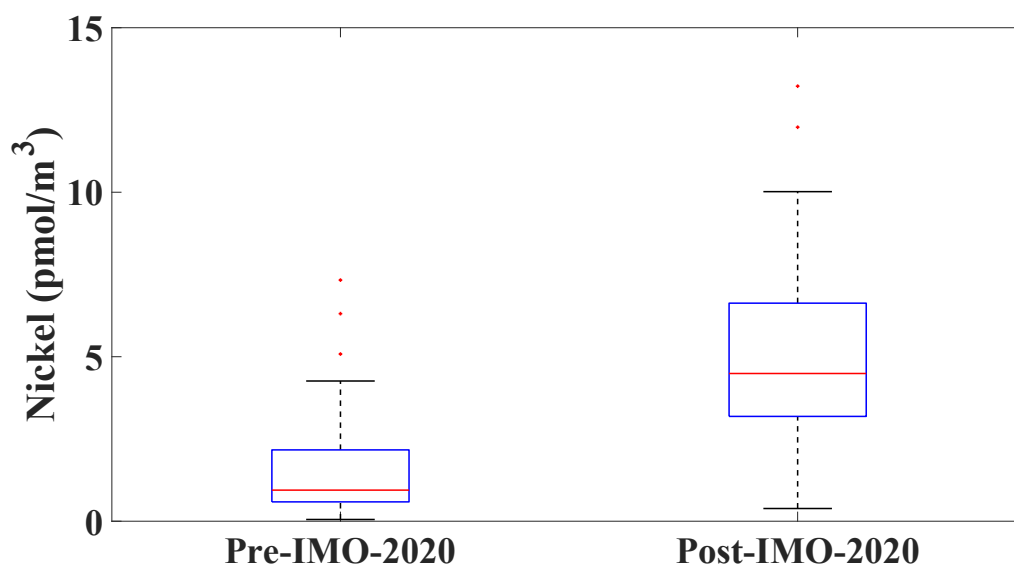
Figure 3.7. Comparison of nickel concentrations pre- and post-IMO-2020 around PPAO

Although considerable similarity between datasets was shown in terms of range, the majority of V datapoints lay in the 0 to 3 pmol/m^3 range pre-IMO-2020, accounting for the greater average. Pre-IMO-2020 concentration for V was greater at 2.9 pmol/m^3 with the datasets showing significant difference ($p<0.05$). From the analysis, atmospheric V concentration around PPAO has reduced in concentration from 2.91 pmol/m^3 to 1.44 pmol/m^3 after the implementation of IMO-2020.

In terms of Ni, significant difference was found with the pre-IMO-2020 dataset from 2015-16, with an increase in Ni concentration from 0.95 pmol/m^3 to 4.8 pmol/m^3 ($p<0.05$). Aside from a small number of samples, pre-IMO-2020 samples were found between 0 and 7.5 pmol/m^3 with post-IMO-2020 samples lying between 2.5 and 10 pmol/m^3. The increase in Ni around PPAO is unexpected but the results could be explained by a larger number of anthropogenically-influenced air masses sampled in the post-IMO-2020 dataset, or fewer pre-IMO-2020, and not necessarily due to increased Ni concentrations in shipping fuel.

While there exists some literature investigating V and Ni changes post-sulfur regulations, the methodologies used consisted of acid-digested aerosol filter samples, thus dissolving a greater percentage of metal constituents within filters. As for the water-soluble fraction of metals, a lesser percentage is dissolved compared to acid-digests, however it is known that for aerosols of anthropogenic origin, metals are more soluble in water than those of crustal origins (Clough et al., 2019, Baker and Jickells, 2017). Therefore, the following comparisons must consider these factors and can be used to gain a general idea of V and Ni changes.

The relative decrease in V is in line with a similar study carried out in China (Yu et al., 2021). In the study, V and Ni concentrations were investigated at a coastal city to determine changes post-IMO-2020. They found a 74% reduction in V after the regulations were implemented, similar to our 50% reduction. However, a decrease in Ni of 18% was also found, compared to a 4-fold increase in the Penlee data. Another study on the effects of the 2015 Chinese 'Fuel Switch at Birth' regulation (reducing sulfur in marine fuels) found that levels of V and Ni in ship exhausts 2 y after the regulation change were only slightly greater than ambient levels (Xiao et al., 2018). This was explained by the analysis of MDO being used by ships in the East China Sea DECA (domestic emission control area), where no V or Ni was detected, compared to V and Ni concentrations in IFOs of over 100 mg kg^{-1} and 50 mg kg^{-1} respectively. In a study carried out in the same area, the implementation of the DECA reduced V levels, with strong correlations found between high S and V content in fuels (Zhang et al., 2019). Zetterdahl et al. (2016) also conducted a study in the North Sea SECA on board a vessel using IMO-2020 compliant residual marine fuel oil (RMB30). Analysis of the oil found 20 % and 6 % of V and Ni concentrations respectively, compared to the concentrations of HFO being used prior to regulation changes (Zetterdahl et al., 2016). With changing V and Ni concentrations in fuels, our study combined with those of others indicates the global aerosol distributions of these elements as markers of shipping emissions has changed.

3.1.6 Is the previous V/Ni ratio valid as a marker of shipping emissions post-IMO-2020?

Figure 3.8 demonstrates that the change to the soluble V/Ni ratio, a strong marker of shipping emissions, has greatly changed in comparison to the pre-IMO-2020 data.
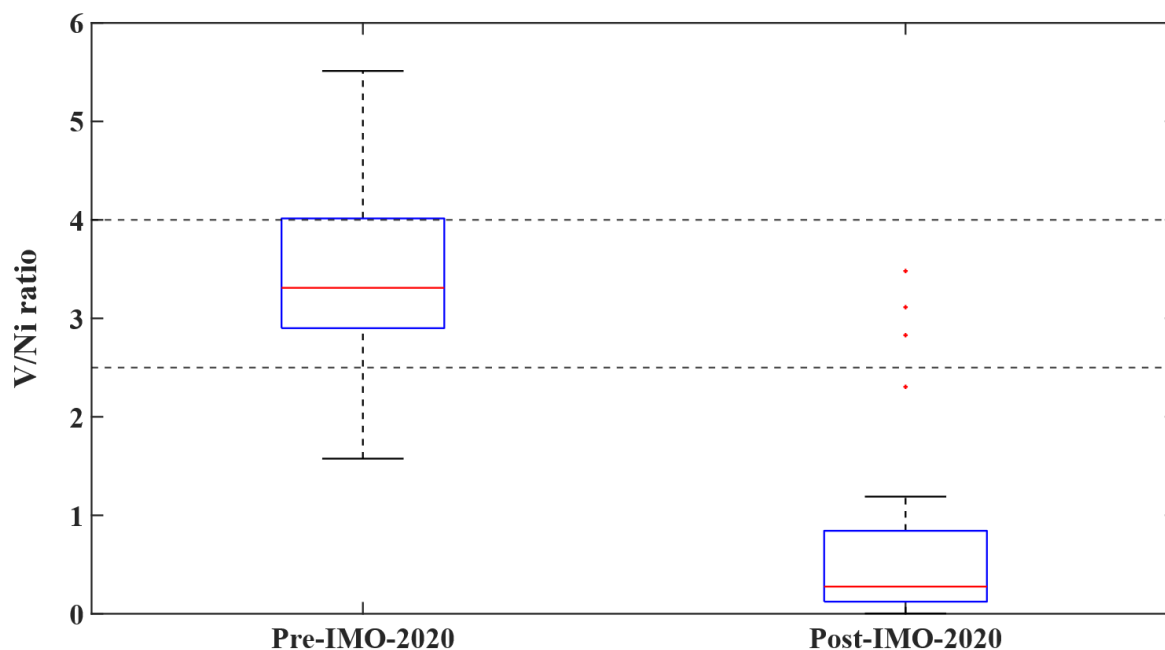
Figure 3.8. Comparison of V/Ni (grams) ratios following IMO-2020 implementation. Horizontal lines represent the previously accepted ratio range of 2.5 to 4 for shipping emissions.

Soluble V/Ni ratios in the post-IMO-2020 dataset were significantly lower than the previous dataset ($p < 0.05$). The decrease in V and increase in Ni concentrations post-IMO-2020 have affected the V/Ni ratio. Pre-IMO-2020, V/Ni ratios lay mostly between 2.5 and 4, consistent with the generally agreed-upon range for shipping emissions (Agrawal et al., 2008, Cesari et al., 2014, Pacyna et al., 2001, Pandolfi et al., 2011). The post-IMO-2020 ratio dropped from 3.3 to 0.28, indicating a significant change in V/Ni ratio using results from the present study. With just 4 samples of 64 having a V/Ni ratio between 2.5 and 4 with the new dataset, there is evidence to conclude that ratios of V/Ni found within ship-emitted aerosols have changed. This

could be a result of new practices implemented by shipping companies to meet IMO-2020 standards, such as additions of scrubbers and changes in fuel types. In comparison with the study by Yu et al. (2021) investigating changes in shipping-emitted V and Ni, a similar trend was observed in the inverse Ni/V ratios. Using the Ni/V ratio, they observed an increase from 0.4 to 2, whereas this study found an increase from 0.4 to 3.6 (Yu et al., 2021)**.**

3.1.7 How do V and Ni concentrations vary across air masses?

Higher soluble V concentrations in the Mainland UK/Ireland and W Europe air masses compared to other sections (1.9 pmol/m^3 and 1.6 pmol/m^3, respectively) are likely attributed to high marine activity in the shipping lane and the high population centres and terrestrial sources of Europe, despite the presence of the North Sea ECA (Visschedijk et al., 2013). The highest concentrations of V, found from the Central Europe air mass (2.6 pmol/m^3) could be due to the combination of ship emissions as well as significant industrial emissions in the area. Such emissions are typically found in the Balkan region originating from oil and petroleum refineries and other industries (Vučković et al., 2013). Soluble Ni showed little variation between sectors, with the Clean Marine air mass having the highest concentration. Although Ni concentrations post-IMO-2020 were significantly greater than those pre-IMO-2020, the consistent concentrations over all sectors indicate a common source. While shipping activity is observed in all sectors, the Atlantic sees much lower marine traffic, yet presented the greatest soluble Ni concentrations. The results could indicate the impact of land-based industries, including emissions from oil combustion in Europe and the UK as well as aerosols transported over the Atlantic from North America.

3.1.8 Correlation between V and Ni

Correlation coefficients were calculated for the soluble metal data. The Spearman's test for correlation was used and found no significant correlation between V and Ni post-IMO-2020.

The scatter plot in Figure 3.9 shows the change from highly correlated V and Ni pre-IMO-2020, to the lack of such post-IMO-2020. The lack of correlation between V and Ni is an indication of a change in shipping emissions of these elements, potentially due to IMO-2020. This is an important observation when considering the situation pre-IMO-2020, where V and Ni were consistently correlated and reflected in the previous V/Ni shipping marker ratio, agreeing with the literature. This finding strengthens the argument that the V/Ni ratio in fuel content has changed, and thus calls into question the V/Ni ratio as a marker.

Another important correlation was found between Sb (a common constituent of marine fuel) with V and Ni ($p<0.05$). Correlations between Ni and Mn and Fe indicate potential dust sources. The correlations with Sb provide evidence of the presence of shipping-emitted aerosols in sampled filters.
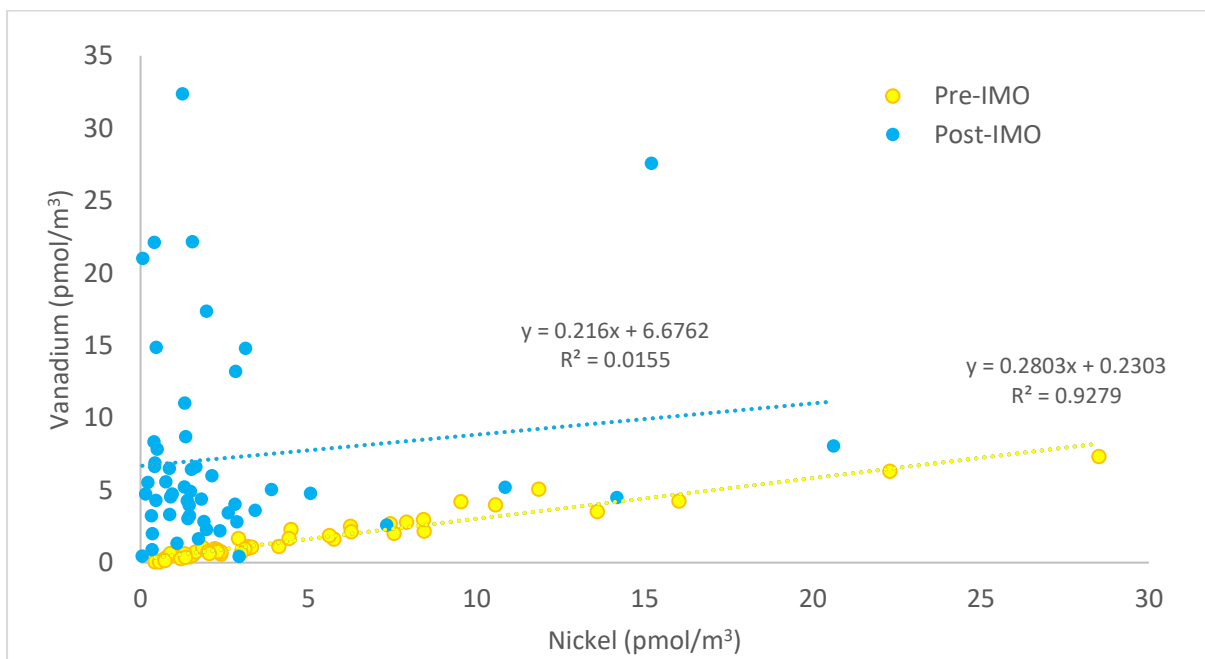

Figure 3.9. Scatter plot of V against Ni pre- and post-IMO-2020.

3.2 Sulfate and soluble major ion aerosol concentrations, pre- and post-IMO-2020 regulations changes

Major ion results from IC analysis were used as a basis for observing the changes in atmospheric sulfur concentrations around PPAO for the two pre- and post-IMO-2020 datasets. The calculated nss-SO_4^{2-} was compared between both datasets as well as within each dataset, investigating distribution over seasons and different air masses. Aerosol filter samples classed as pre-IMO-2020 from 2017-18 (n=61) were compared to post-IMO-2020 samples from 2019-21 (n=43).

Air mass sector classifications were considered when comparing datasets. Changes in nss-SO_4^{2-} within the Unregulated Shipping air mass, due to the influence of shipping emissions on air masses, could be attributed to IMO-2020. For the remaining sectors, the changes could not solely be attributed to the IMO regulation. The number of Unregulated Shipping samples are only 9 and 17 in number for pre- and post-IMO respectively, and seasonal variations in nss-SO_4^{2-} must also be considered due to the presence of natural DMS production in the marine atmosphere.

3.2.1 Have nss-SO_4^{2-} concentrations in air masses arriving at PPAO changed since the regulation change?

Figure 3.10 compares the concentration distributions of each dataset. Lower nss-SO_4^2 concentrations are clearly seen post-regulation and are significantly different to pre-IMO-2020 using the MW-U test (p<0.05). nss-SO_4^{2-} concentration dropped from 1.4 to 0.3 µg/m^3.

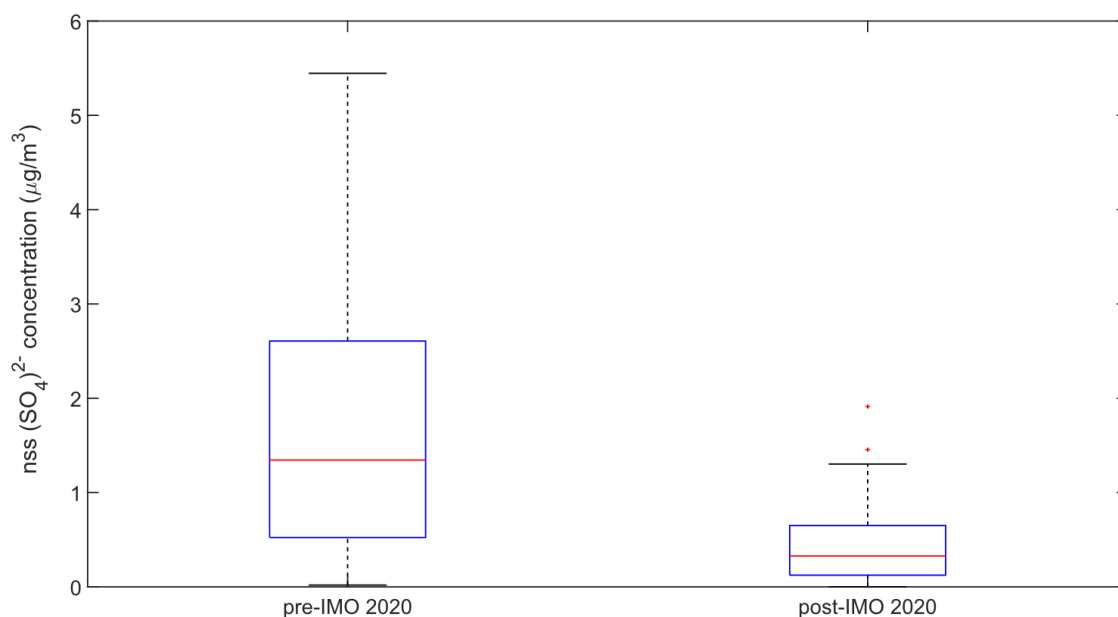Figure 3.10. nss-SO_4^{2-} distribution pre- and post-IMO-2020.

Post-IMO-2020 nss-SO_4^{2-} concentrations lay consistently in the range of 0-2 µg/m³, with the exception of one outlier. In comparison, nss-SO_4^{2-} concentrations around PPAO before 2020 mostly ranged between 0-3 µg/m³, with multiple datapoints reaching up to 14 µg/m³. Given the location of the sampling of the study, reduced SO_4^{2-} emissions as a result of shipping traffic are expected from IMO-2020 changes. In areas inland and/or further from shipping activity, clear decreases in nss-SO_4^{2-} might not be observed due to more abundant alternative sources of the pollutant but such a change in atmospheric chemical composition in coastal regions could be reasonable.

3.2.2 How do the air mass distributions compare between datasets?

The number of samples per air mass classification vary between the two datasets. Significantly greater nss-SO_4^{2-} concentrations were observed across all air masses pre-regulation compared to post-IMO-2020 ($p < 0.05$). Average comparisons by air mass are seen below in Figure 3.11, with differences in average concentrations clearly visible.
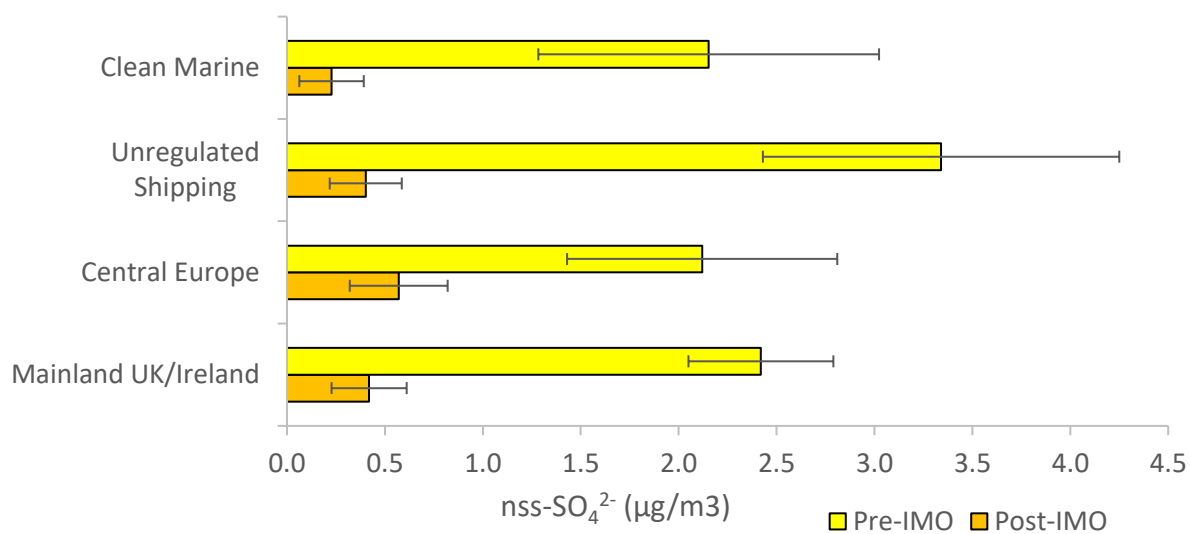
Figure 3.11. Mean average nss-SO_4^{2-} concentrations pre- and post-IMO-2020 split by air mass classification with error bars (use of mean average due to low sample number in comparison groups).

Interestingly, no significant differences were found between any air mass for the pre-IMO-2020 regulation dataset ($p > 0.05$). Figure 3.12 reflects the similarity in nss-SO_4^{2-} between air masses, with no clear differences in character. Also, the post-IMO-2020 dataset did not find any significant difference between air masses ($p > 0.05$). Although averages were similar, the similarity between air mass nss-SO_4^{2-} concentrations could be explained by less frequent high nss-SO_4^{2-} events. These results indicate that, at least for the datasets investigated, the analysis of filter samples cannot be used to distinguish chemical differences in air masses.
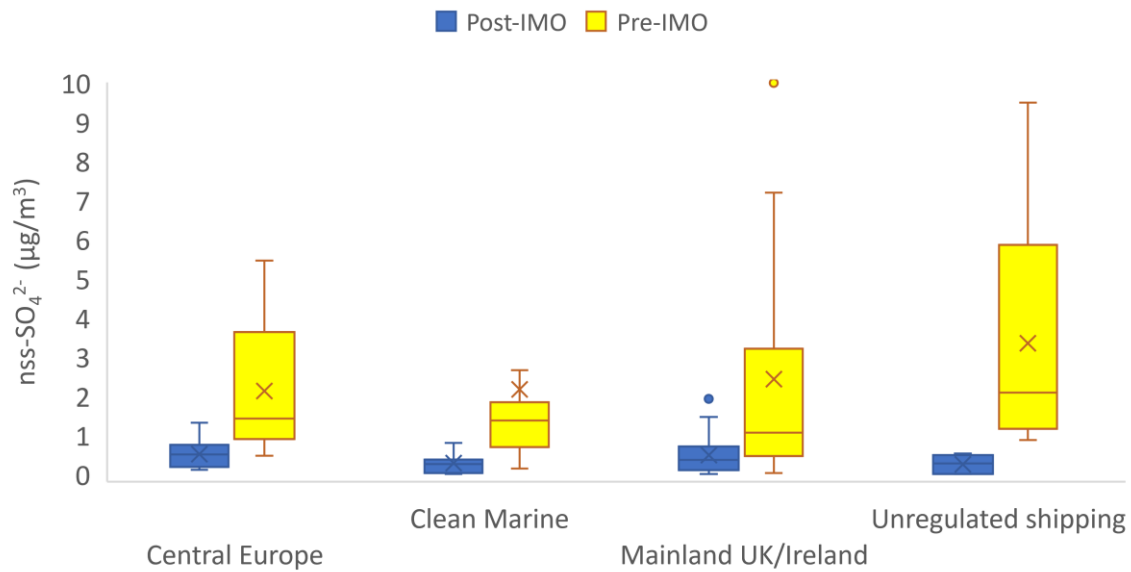
Figure 3.12. Pre- and post-IMO-2020 nss-SO_4^{2-} split by air mass classifications.

3.2.3 How do seasonal variations of nss-SO_4^{2-} compare between datasets?

Clear variations in nss-SO_4^{2-} by seasons were observed post-IMO-2020. The spring and summer seasons were significantly greater than autumn and winter ($p<0.05$), with Figure 3.13 in showing the fluctuation.
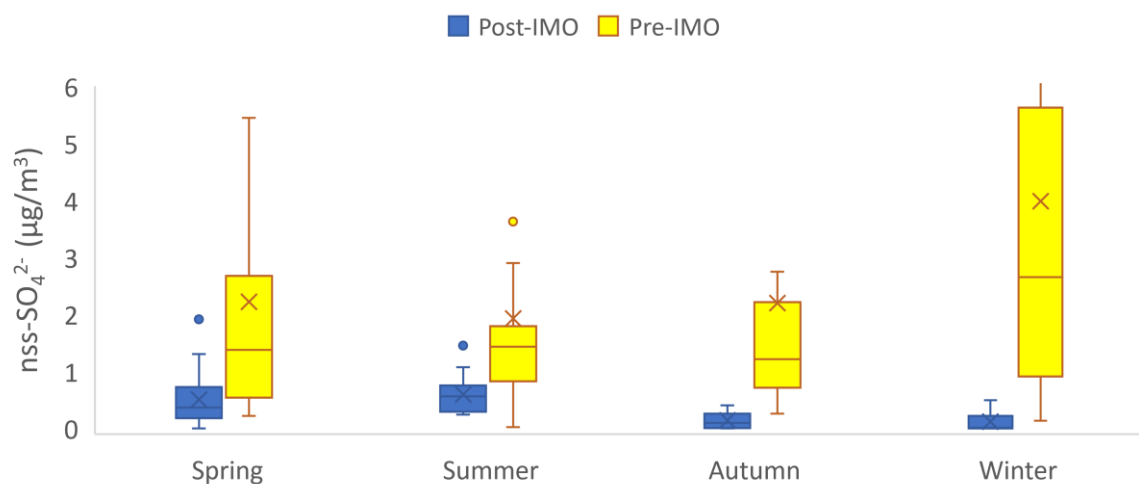
Figure 3.13. Pre- and post-IMO-2020 seasonal nss-SO_4^{2-} variation. Upper whiskey for pre-IMO winter (7.19) hidden for scale. 'x' symbol represents mean with central line representing median.

Differences in average seasonal concentration for both pre- and post-IMO-2020 are found in Figure 3.14. Revisiting the variation in nss-SO_4^{2-} over time in 3.9, a clearly visible increase in the spring and summer seasons is shown followed by a decrease after these periods, and this is reflected in the average seasonal concentrations. A strong argument of major change to atmospheric chemistry in the region can be made since it appears that natural DMS production dominated nss-SO_4^{2-} concentrations in the marine atmosphere around PPAO, compared to the pre-IMO-2020 dataset which showed constant and much higher nss-SO_4^{2-} throughout all seasons. Although, it must be noted that due to a greater number of sampled Unregulated Shipping air masses, and comparison of seasonal variations pre- and post-regulation must take this into account.

Figure 3.14. Mean average seasonal concentrations of nss-SO_4^{2-} pre- and post-IMO-2020 with error bars (use of mean due to low sample numbers in comparison groups).

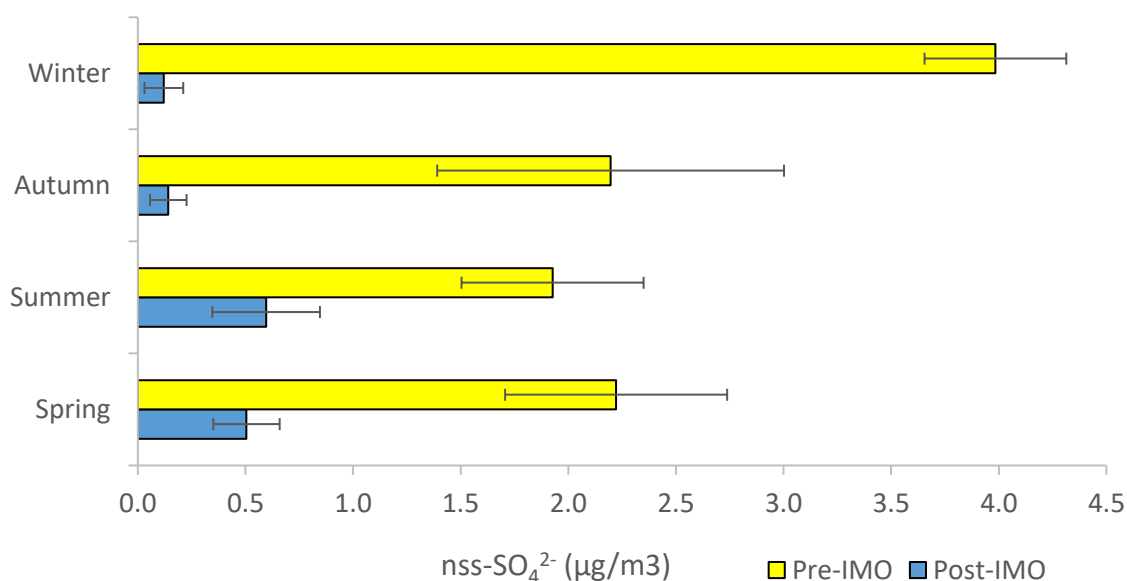In contrast, data from the pre-IMO-2020 period showed no seasonal variation in nss-SO_4^{2-} ($p<0.05$). Concentrations were relatively stable over seasons, as seen in Figure 3.13. It is apparent that for the pre-IMO-2020 dataset, DMS production was not a main factor affecting marine atmospheric nss-SO_4^{2-}.

The possibility of changing contributions of DMS production between the two datasets must be considered when using nss-SO_4^{2-} to investigate the effect of the IMO regulation on marine atmospheric sulfur. If it was the case that spring and summer nss-SO_4^{2-} concentrations were greater post-IMO, it could possibly be attributed to DMS production. However, it is unlikely that the difference in concentrations could be due to an increased DMS signal.

3.2.4 Potential limitations of this study

The results are accompanied by uncertainties for various reasons, mainly mathematical uncertainties calculated from the IC analysis as well as theoretical uncertainties and low sample numbers. The widely used method of subtraction of ss-SO_4^{2-} from total SO_4^{2-} using the typical chemical composition of sea salt can often introduce great uncertainty. With the potential presence of foreign nss-Na^+, this calculation can often underestimate nss-SO_4^{2-} as depicted by the negative values in this study. However, high uncertainties are only found for a small proportion of the data allowing important trends elucidated and comparisons to be made.

The slight difference in sampling method, i.e. the use of fraction-separation with a cascade impactor for the current project rather than just a filter, could possibly bias major ion concentrations from the restriction of flow rate through the filter. Although, the equipment and processing were the same apart from this and the interpretation due to a change in sampling strategy has been taken into account.

The methodology for deciding air mass classifications introduces some uncertainties that need consideration. Classified air masses often passed over multiple sectors leading to mixing, thus affecting chemical composition of aerosols. The weighting applied to Clean Marine samples

helped in classifying these 'pristine' samples properly; however, the limitations of the methodology as a whole must be considered in the sector analysis results.

The impact of restrictions set in place to reduce the spread of the COVID-19 pandemic must also be considered. Reductions in maritime activity, and the consequent reduction in shipping emissions, could have affected concentrations of V, Ni and nss-SO_4^{2-} in samples taken during the most intense lockdown periods (e.g. March to July, 2020). In terms of the comparison of pre- and post-IMO-2020 values, reductions in atmospheric concentrations could be attributed to reduced shipping activity. A study using AIS data found global changes of +2.3 to -13.8% in container, dry bulk and wet bulk shipping activity, alongside reductions in passenger traffic between 19.6 and 42.8% (Millefiori et al., 2021). A similar study estimated total global maritime trade to have reduced by up to 9.6% (Verschuur et al., 2021). An AIS-based study on six locations with high shipping activity found a total decrease in traffic occupancy of 1.4% (including a maximum reduction of passenger ship activity of 30% (March et al., 2021). The study also found a peak reduction in shipping activity around the UK of 11%. The marine-activity based estimations of reductions in maritime activity suggest that in general, maritime activity did not drop substantially enough to significantly affect the results found in this study. Nevertheless, the added uncertainty from the COVID-19 pandemic is something which should be taken into account.

With respect to the data quality, cases with very high uncertainties were attributed to missing repeat measurements of aerosol filters, either due to instrumental IC errors or to the removal of a singular measurement with substantially higher or lower concentrations than remaining injections. Negative nss-SO_4^{2-} values are also observed for the samples carried out during the current project, most of which are accompanied by high uncertainties. The results can be explained by the nss-SO_4^{2-} correction using sodium and sulfate with the standard chemical composition of sea water as a reference. The assumption provided by the correction does not

consider foreign nss-Na^+, which can lead to an over-estimation of ss-SO_4^{2-} which is then removed from the equation. An argument could also be made for the deposition and subsequent crystallisation of sea salt onto foreign surfaces (such as sand and soil), thus changing sea salt composition based on the place of deposition. In these cases, once the sea-salt crystals are transported by wind onto the filter, the applied mathematical corrections cannot be used reliably. Overall, nss-SO_4^{2-} concentrations have decreased based on the datasets analysed.

Chapter 4. Conclusions and future work

This unique project gives an insight into the change of aerosol chemical character with a focus on nss-sulfate and V/Ni ratios from shipping post-IMO-2020, the latter often used as a marker of shipping emissions. As a result of the change in V and Ni, it is apparent that the ratio has significantly changed in local UK waters and North Western Europe with Ni covarying with other metals such as Cd, Zn, Co, Cr and Cu, indicating other sources of V unrelated to shipping activity. Meanwhile, the reduction in soluble V has indicated a potential decrease in shipping-related atmospheric V emissions, while covarying with only Zn and Sb. This supports data from other studies that the previously accepted 2.5-4 V/Ni range will no longer be a sensitive tracer of shipping emissions. It is clear that with changing fuel types with varying V and Ni concentrations, shipping emissions have undergone a change in chemical character.

The data from major ion analysis indicated reductions in nss-SO_4^{2-} around Penlee Point Atmospheric Observatory in Southwest England. This decrease, although perhaps not to the same magnitude as indicated in this study, is very plausible due to the location of the sample site and its exposure to ship exhaust fumes from marine vessels traversing the English Channel and the Atlantic Ocean. As the IMO-2020 regulation reduced shipping fuel sulfur concentration 7-fold, it is likely that atmospheric sulfur has decreased in regions of high marine traffic. Additionally, when considering the transboundary aerosol transport of sulfate, the regulation could improve air quality worldwide, not solely in coastal regions.

In terms of the change in seasonal fluctuation of nss-SO_4^{2-} observed at PPAO, an interesting inference could be made. Pre-IMO-2020, we saw a marine atmosphere potentially saturated with nss-SO_4^{2-}. Post-IMO-2020, however, the results showed a purely DMS-dominated atmosphere. With decreased nss-SO_4^{2-} around PPAO (possibly due to the IMO-2020 sulfur

regulation), the observatory would be able to track seasonal DMS fluctuation as opposed to shipping-related sulfur emissions.

Crucially, the potential positive effect on air quality could substantially reduce sulfur-induced health problems in coastal and land-locked communities. The overall reduction in atmospheric sulfur from the shipping industry indicates that the IMO-2020 regulation has made a positive change towards better air quality.

Recommended future work would focus on fuel chemistry and marine ambient concentrations in order to gain a clearer understanding of the effects of the IMO-2020 regulation on trace element emissions. In terms of sampling campaigns tracking such changes in shipping regulations, high-time resolution samples over a long duration is necessary for strong results. The use of real-time online measurements can eliminate the need for collection and subsequent analysis of aerosol filters; however, this range of equipment is costly. For a deeper investigation of sulfur, isotope analysis (using techniques such as Isotope Ratio Mass Spectrometry) can uncover specific sources of sulfur, adding a new layer of information to $nss\text{-}SO_4^{2-}$ results. The use of isotope analysis has proven effective in distinguishing between sulfur emission sources in marine aerosols (Lin et al., 2012).

Further, chemical analyses of marine fuels and onboard exhaust-gas measurements are needed to track and predict the effect of shipping emissions on the atmosphere. Through the analysis of newer LSFOs, predictions for emissions of these fuels can be made. Smokestack analyses can also provide crucial information on ship exhaust emissions before dispersing in the atmosphere.

Reference list

AGRAWAL, H., MALLOY, Q. G. J., WELCH, W. A., WAYNE MILLER, J. & COCKER, D. R. 2008. In-use gaseous and particulate matter emissions from a modern ocean going container vessel. Atmospheric Environment (1994), 42, 5504-5510.

AKSOYOGLU, S., BALTENSPERGER, U. & PRÉVÔT, A. S. H. 2016. Contribution of ship emissions to the concentration and deposition of air pollutants in Europe. Atmospheric Chemistry and Physics, 16, 1895-1906.

ALEMÓN, E., HERRERA, L., ORTIZ, E. & LONGORIA, L. C. 2004. Instrumental nuclear activation analysis (INAA) characterization of environmental air filter samples. Appl Radiat Isot, 60, 815-823.

AMOATEY, P., OMIDVARBORNA, H., BAAWAIN, M. S. & AL-MAMUN, A. 2019. Emissions and exposure assessments of SOX, NOX, PM10/2.5 and trace metals from oil industries: A review study (2000–2018). Process Safety and Environmental Protection, 123, 215-228.

ANDERSON, H. R., SPIX, C., MEDINA, S., SCHOUTEN, J. P., CASTELLSAGUE, J., ROSSI, G., ZMIROU, D., TOULOUMI, G., WOJTYNIAK, B., PONKA, A., BACHAROVA, L., SCHWARTZ, J. & KATSOUYANNI, K. 1997. Air pollution and daily admissions for chronic obstructive pulmonary disease in 6 European cities: results from the APHEA project. Eur Respir J, 10, 1064-1071.

ANSARI, T. M., MARR, I. L. & TARIQ, N. 2004. Heavy Metals in marine pollution perspective–a mini review. Journal of Applied Sciences, 4, 1-20.

APARICIO-GONZALEZ A., DUARTE C. M. & TOVAR-SANCHEZ A. 2012. Trace metals in deep ocean waters: A review. Journal of Marine Systems 100-101, 26-33.

ASSI, M. A., HEZMEE, M. N. M., HARON, A. W., SABRI, M. Y. M. & RAJION, M. A. 2016. The detrimental effects of lead on human and animal health. Vet World, 9, 660-671.

ATILHAN, S., PARK, S., EL-HALWAGI, M. M., ATILHAN, M., MOORE, M. & NIELSEN, R. B. 2021. Green hydrogen as an alternative fuel for the shipping industry. Current Opinion in Chemical Engineering, 31, 100668.

BASUMALLICK, L. R., JEFFREY 2016. Ion chromatography assay for chloride and sulfate in adenosine. Thermo Fisher Library.

BAKER, A. R. & JICKELLS, T. D. 2017. Atmospheric deposition of soluble trace elements along the Atlantic Meridional Transect (AMT). Progress in Oceanography 2017, 158, 41-51.

BEECKEN, J., MELLQVIST, J., SALO, K., EKHOLM, J. & JALKANEN, J. P. 2014. Airborne emission measurements of SO2, NOx and particles from individual ships using a sniffer technique. Atmospheric Measurement Techniques, 7, 1957-1968.

BYEON, S.-H., WILLIS, R. & PETERS, T. M. 2015. Chemical characterization of outdoor and subway fine (PM(2.5-1.0)) and coarse (PM(10-2.5)) particulate matter in Seoul (Korea) by computer-controlled scanning electron microscopy (CCSEM). Int J Environ Res Public Health, 12, 2090-2104.

CAMPLING, P. J., LILIANE; VANHERLE, KRIS; COFALA, JANUSZ; HEYES, CHRIS; SANDER, ROBERT 2013. Specific evaluation of emissions from shipping including assessment for the establishment of possible new emission control areas in European Seas.

CARMICHAEL, G. R., STREETS, D. G., CALORI, G., AMANN, M., JACOBSON, M. Z., HANSEN, J. & UEDA, H. 2002. Changing Trends in Sulfur Emissions in Asia: Implications for Acid Deposition, Air Pollution, and Climate. Environmental. Science. Technology, 36, 4707-4713.

CESARI, D., GENGA, A., IELPO, P., SICILIANO, M., MASCOLO, G., GRASSO, F. M. & CONTINI, D. 2014. Source apportionment of PM2.5 in the harbour–industrial area of Brindisi (Italy): Identification and estimation of the contribution of in-port ship emissions. The Science of the Total Environment, 497-498, 392-400.

CHANDRA MOULI, P., VENKATA MOHAN, S. & JAYARAMA REDDY, S. 2003. A study on major inorganic ion composition of atmospheric aerosols at Tirupati. J Hazard Mater, 96, 217-228.

CHEN, D., FU, X., GUO, X., LANG, J., ZHOU, Y., LI, Y., LIU, B. & WANG, W. 2020. The Impact of Ship Emissions on Nitrogen and Sulfur Deposition in China. Science of the Total Environment, 708.

CHEN, D., TIAN, X., LANG, J., ZHOU, Y., LI, Y., GUO, X., WANG, W. & LIU, B. 2019. The impact of ship emissions on PM.sub.2.5 and the deposition of nitrogen and sulfur in Yangtze River Delta, China. The Science of the Total Environment, 649, 1609.

CHEN, D., WANG, X., LI, Y., LANG, J., ZHOU, Y., GUO, X. & ZHAO, Y. 2017. High-spatiotemporal-resolution ship emission inventory of China based on AIS data in 2014. Sci Total Environ, 609, 776-787.

CHEN, Q., SHERWEN, T., EVANS, M. & ALEXANDER, B. 2018. DMS oxidation and sulfur aerosol formation in the marine troposphere: a focus on reactive halogen and multiphase chemistry. Atmospheric Chemistry and Physics, 18, 13617-13637.

CHEN, R., HUANG, W., WONG, C.-M., WANG, Z., QUOC THACH, T., CHEN, B. & KAN, H. 2012. Short-term exposure to sulfur dioxide and daily mortality in 17 Chinese cities: The China air pollution and health effects study (CAPES). Environ Res, 118, 101-106.

CHENG, Y., WANG, S., ZHU, J., GUO, Y., ZHANG, R., LIU, Y., ZHANG, Y., YU, Q., MA, W. & ZHOU, B. 2019. Surveillance of SO2 and NO2 from ship emissions by MAX-DOAS measurements and the implications regarding fuel sulfur content compliance. Atmospheric Chemistry and Physics, 19, 13611-13626.

CHESTER, R. J., TIM D. 1990. Marine Geochemistry.

CHIANESE, E., TIRIMBERIO, G., APPOLLONI, L., DINOI, A., CONTINI, D., DI GILIO, A., PALMISANI, J., COTUGNO, P., MINIERO, D. V., DUSEK, U., CAMMINO, G. & RICCIO, A. 2022. Chemical characterisation of PM10 from ship emissions: a study on samples from hydrofoil exhaust stacks. Environmental Science and Pollution Research, 29, 17723-17736.

CHOJNACKA, K., SAMORAJ, M., TUHY, Ł., MICHALAK, I., MIRONIUK, M. & MIKULEWICZ, M. 2018. Using XRF and ICP-OES in biosorption studies. Molecules, 23, 2076.

CHU VAN, T., RAMIREZ, J., RAINEY, T., RISTOVSKI, Z. & BROWN, R. J. 2019. Global impacts of recent IMO regulations on marine fuel oil refining processes and ship emissions. Transportation research. Part D, Transport and Environment, 70, 123-134.

CLAREMAR, B., HAGLUND, K. & RUTGERSSON, A. 2017. Ship emissions and the use of current air cleaning technology: contributions to air pollution and acidification in the Baltic Sea. Earth System Dynamics, 8, 901-919.

CLOUGH, R., LHAN, M. C., USSHER, S. J., NIMMO, M & WORSFELD, P.J. 2019. Uncertainty associated with the leaching of aerosol filters for the determination of metals in aerosol particulate matter using collision/reaction cell ICP-MS detection. Talanta 2019 Vol. 199, 425-430.

CORBETT, J. J., FISCHBECK, P. S. & PANDIS, S. N. 1999. Global nitrogen and sulfur inventories for oceangoing ships. Journal of Geophysical Research: Atmospheres, 104, 3457-3470.

CORBIN, J. C., MENSAH, A. A., PIEBER, S. M., ORASCHE, J., MICHALKE, B., ZANATTA, M., CZECH, H., MASSABÒ, D., BUATIER DE MONGEOT, F., MENNUCCI, C., EL HADDAD, I., KUMAR, N. K., STENGEL, B., HUANG, Y., ZIMMERMANN, R., PRÉVÔT, A. S. H. & GYSEL, M. 2018. Trace metals in soot and PM2.5 from heavy-fuel-oil combustion in a marine engine. Environmental. Science. Technology, 52, 6714-6722.

CURTIS, L., REA, W., SMITH-WILLIS, P., FENYVES, E. & PAN, Y. 2006. Adverse health effects of outdoor air pollutants. Environ Int, 32, 815-830.

DENIZ, C. & DURMUŞOĞLU, Y. 2008. Estimating shipping emissions in the region of the Sea of Marmara, Turkey. Sci Total Environ, 390, 255-261.

DENIZ, C. & ZINCIR, B. 2016. Environmental and economical assessment of alternative marine fuels. Journal of Cleaner Production, 113, 438-449.

DING, A., HUANG, X., NIE, W., CHI, X., XU, Z., ZHENG, L., XIE, Y., QI, X., SHEN, Y., SUN, P., WANG, J., WANG, L., SUN, J., YANG, X. Q., QIN, W., ZHANG, X., CHENG, W., LIU, W., PAN, L. & FU, C. 2019. Significant reduction of PM2.5 in eastern China due to regional-scale emission control: evidence from SORPES in 2011–2018. Atmospheric Chemistry and Physics, 19, 11791-11801.

DORE, A., VIENO, M., TANG, Y., DRAGOSITS, U., DOSIO, A., WESTON, K. & SUTTON, M. 2007. Modelling the atmospheric transport and deposition of sulphur and

nitrogen over the United Kingdom and assessment of the influence of SO2 emissions from international shipping. Atmospheric Environment (1994), 41, 2355-2367.

ELGOHARY, M. M., SEDDIEK, I. S. & SALEM, A. M. 2015. Overview of alternative fuels with emphasis on the potential of liquefied natural gas as future marine fuel. Proceedings of the Institution of Mechanical Engineers. Part M, Journal of Engineering for the Maritime Environment, 229, 365-375.

EPA 2019. US Environmental Protection Agency, what is acid rain?

EYRING, V., ISAKSEN, I. S. A., BERNTSEN, T., COLLINS, W. J., CORBETT, J. J., ENDRESEN, O., GRAINGER, R. G., MOLDANOVA, J., SCHLAGER, H. & STEVENSON, D. S. 2010. Transport impacts on atmosphere and climate: Shipping. Atmospheric Environment (1994), 44, 4735-4771.

FAN, Q., ZHANG, Y., MA, W., MA, H., FENG, J., YU, Q., YANG, X., NG, S. K. W., FU, Q. & CHEN, L. 2016. Spatial and seasonal dynamics of ship emissions over the Yangtze River Delta and East China Sea and their potential environmental influence. Environ. Sci. Technol, 50, 1322-1329.

FOSCO, T. & SCHMELING, M. 2007. Determination of water-soluble atmospheric aerosols using ion chromatography. Environ Monit Assess, 130, 187-199.

FUNG, K. M., HEALD C., KROLL J. H., WANG S., JO D. S., GETELMAN A., LU Z., LIU X., ZAVERI R. A., APEL E. C., BLAKE D. R., JIMENEZ J. L., CAMPUZANO-JOST P., VERES P. R., BATES T. S., SHILLING J. E. & ZAWADOWICZ M. 2022 Exploring dimethyl sulfide (DMS) oxidation and implications for global aerosol radiative forcing. Atmospheric Chemistry and Physics 22, 1549-1573.

FURGER, M., MINGUILLÓN, M. C., YADAV, V., SLOWIK, J. G., HÜGLIN, C., FRÖHLICH, R., PETTERSON, K., BALTENSPERGER, U. & PRÉVÃ´T, A. S. H. 2017. Elemental composition of ambient aerosols measured with high temporal resolution using an online XRF spectrometer. Atmospheric Measurement Techniques, 10, 2061-2076.

GEORGE, M., OSMAN, A. S. S., HUSSIN, H. & GEORGE, A. R. 2017. Protecting the Malacca and Singapore Straits from ships' atmospheric emissions through the implementation of MARPOL Annex vi. The International Journal of Marine and Coastal Law, 32, 95-137.

GILBERT, P., WALSH, C., TRAUT, M., KESIEME, U., PAZOUKI, K. & MURPHY, A. 2018. Assessment of full life-cycle air emissions of alternative shipping fuels. Journal of Cleaner Production, 172, 855-866.

GOLDSWORTHY, L. & GOLDSWORTHY, B. 2015. Modelling of ship engine exhaust emissions in ports and extensive coastal waters based on terrestrial AIS data – An Australian case study. Environmental Modelling & Software: with Environment Data News, 63, 45-60.

GOUDARZI, G., GERAVANDI, S., IDANI, E., HOSSEINI, S. A., BANESHI, M. M., YARI, A. R., VOSOUGHI, M., DOBARADARAN, S., SHIRALI, S., MARZOONI, M. B., GHOMEISHI, A., ALAVI, N., ALAVI, S. S. & MOHAMMADI, M. J. 2016. An evaluation of hospital admission respiratory disease attributed to sulfur dioxide ambient concentration in Ahvaz from 2011 through 2013. Environ Sci Pollut Res Int, 23, 22001-22007.

GRAY, B. A., WANG, Y., GU, D., BANDY, A., MAULDIN, L., CLARKE, A., ALEXANDER, B. & DAVIS, D. D. 2011. Sources, transport, and sinks of SO2 over the equatorial Pacific during the Pacific Atmospheric Sulfur Experiment. Journal of Atmospheric Chemistry, 68, 27-53.

GREAVER, T. L., SULLIVAN, T. J., HERRICK, J. D., BARBER, M. C., BARON, J. S., COSBY, B. J., DEERHAKE, M. E., DENNIS, R. L., DUBOIS, J.-J. B., GOODALE, C. L., HERLIHY, A. T., LAWRENCE, G. B., LIU, L., LYNCH, J. A. & NOVAK, K. J. 2012. Ecological effects of nitrogen and sulfur air pollution in the US: what do we know? Frontiers in Ecology and the Environment, 10, 365-372.

HALFF, A., YOUNES, L. & BOERSMA, T. 2019. The likely implications of the new IMO standards on the shipping industry. Energy Policy, 126, 277-286.

HASSELÖV, I.-M., TURNER D. R., LAUER A. & CORBETT J. J. 2013. Shipping contributes to ocean acidification. Geophysical Research Letters 40, 2731-2736.

HILL, C. R., SHAFAEI A., BALMER L., LEWIS J. R., HODGSON J. M., MILLAR A. H. & BLEKKENHORST L. C. 2022 Sulfur compounds: From plants to humans and their role in chronic disease prevention. Critical Reviews in Food Science and Nutrition

HONGISTO, M. & SOFIEV M. 2004. Long-range transport of dust to the Baltic Sea region. International Journal of Environment and Pollution 22, 72-86

HUANG, J., ZHOU, K., ZHANG, W., LIU, J., DING, X., CAI, X. A. & MO, J. 2019. Sulfur deposition still contributes to forest soil acidification in the Pearl River Delta, South China, despite the control of sulfur dioxide emission since 2001. Environ Sci Pollut Res Int, 26, 12928-12939.

ICCT 2017. Greenhouse Gas Emissions from Global Shipping, 2013-2015.

IEA (2016). WEO-2016 Special Report: Energy and Air Pollution, International Energy Agency Paris, France.

IM, U., CHRISTODOULAKI, S., VIOLAKI, K., ZARMPAS, P., KOCAK, M., DASKALAKIS, N., MIHALOPOULOS, N. & KANAKIDOU, M. 2013. Atmospheric deposition of nitrogen and sulfur over southern Europe with focus on the Mediterranean and the Black Sea. Atmospheric Environment (1994), 81, 660-670.

IMO 2005. MARPOL Annex VI.

IMO 2014a. Sulphur Oxides (SOx) - Regulation 14.

IMO 2014b. Third IMO GHG Study.

IMO 2016. Study on effects of the entry into force of the global 0.5% fuel oil sulphur content limit on human health.

IMO 2018. IMO GHG strategy.

IMO. 2019a. IMO 2020 - Cutting Sulphur Oxide Emissions [Online]. [Accessed].

IMO. 2019b. International Convention for the Prevention of Pollution from Ships (MARPOL) [Online]. [Accessed].

JAHAN, S. & STREZOV, V. 2019. Assessment of trace elements pollution in the sea ports of New South Wales (NSW), Australia using oysters as bioindicators. Sci Rep, 9, 1416-1416.

JALKANEN, J. P., JOHANSSON, L. & KUKKONEN, J. 2016. A comprehensive inventory of ship traffic exhaust emissions in the European sea areas in 2011. Atmospheric Chemistry and Physics, 16, 71-84.

JI-MING, H. A. O., SHU-XIAO, W., BING-JIANG, L. I. U. & KE-BIN, H. E. 2000. Control strategy for sulfur dioxide and acid rain pollution in China. Journal of Environmental Sciences (China), 12, 385-393.

JI, J. S. 2020. The IMO 2020 sulphur cap: a step forward for planetary health? Lancet Planet Health, 4, e46-e47.

JOHANSSON, L., JALKANEN, J.-P. & KUKKONEN, J. 2017. Global assessment of shipping emissions in 2015 on a high spatial and temporal resolution. Atmospheric Environment (1994), 167, 403-415.

JOMOVA, K., JENISOVA, Z., FESZTEROVA, M., BAROS, S., LISKA, J., HUDECOVA, D., RHODES, C. J. & VALKO, M. 2011. Arsenic: toxicity, oxidative stress and human disease: Toxicity of arsenic. Journal of Applied Toxicology, n/a.

KAMPA, M. & CASTANAS, E. 2008. Human health effects of air pollution. Environ Pollut, 151, 362-367.

KIM, C. H., PARK S. Y., KIM Y. J., CHANG L. S., SONG S. K., MOON Y. S. & SONG C. K., 2012. A numerical study on indicators of long-range transport potential for anthropogenic particulate matters over northeast Asia. Atmospheric Environment 58, 35-44.

KINDAP, T., UNAL A., CHEN S. H., HU Y., ODMAN M. T. & KARACA M. 2006. Long-range aerosol transport from Europe to Istanbul, Turkey. Atmospheric Environment 40, 3536-3547.

KONTOVAS, C. A. 2020. Integration of air quality and climate change policies in shipping: The case of sulphur emissions regulation. Marine Policy, 113, 103815.

KOTCHENRUTHER, R. A. 2015. The effects of marine vessel fuel sulfur regulations on ambient PM2.5 along the west coast of the U.S. Atmospheric Environment (1994), 103, 121-128.

KOTCHENRUTHER, R. A. 2017. The effects of marine vessel fuel sulfur regulations on ambient PM2.5 at coastal and near coastal monitoring sites in the U.S. Atmospheric Environment (1994), 151, 52-61.

LECK, C. & PERSSON, C. 1996. Seasonal and short-term variability in dimethyl sulfide, sulfur dioxide and biogenic sulfur and sea salt aerosol particles in the arctic marine boundary layer during summer and autumn. Tellus. Series B, Chemical and Physical Meteorology, 48, 272-299.

LEE, R. E. & VON LEHMDEN, D. J. 1973. Trace Metal Pollution in the Environment. Journal of the Air Pollution Control Association, 23.

LEE, S., KIM, J., CHOI, M., HONG, J., LIM, H., ECK, T. F., HOLBEN, B. N., AHN, J.-Y., KIM, J. & KOO, J.-H. 2019. Analysis of long-range transboundary transport (LRTT) effect on Korean aerosol pollution during the KORUS-AQ campaign. Atmospheric Environment (1994), 204, 53-67.

LI, C., YUAN, Z., OU, J., FAN, X., YE, S., XIAO, T., SHI, Y., HUANG, Z., NG, S. K. W., ZHONG, Z. & ZHENG, J. 2016. An AIS-based high-resolution ship emission inventory and its uncertainty in Pearl River Delta region, China. Sci Total Environ, 573, 1-10.

LIKUS-CIEŚLIK, J., SOCHA, J., GRUBA, P. & PIETRZYKOWSKI, M. 2020. The current state of environmental pollution with sulfur dioxide (SO2) in Poland based on sulfur concentration in Scots pine needles. Environ Pollut, 258, 113559.

LIN, C.-Y., LIU S. C., CHOU C. C. K., HUANG S. J, LIU C. M., KUO C. H. & YOUNG C. Y. 2005. Long-range transport of aerosols and their impact on the air quality of Taiwan. Atmospheric Environment 39, 6066-6076.

LIN, C. T., BAKER A. R., JICKELLS T. D., KELLY S. & LESWORTH T. 2012. An assessment of the significance of sulphate sources over the Atlantic Ocean based on sulphur isotope data. Atmospheric Environment 62, 615-621.

LIN, H., TAO, J., QIAN, Z., RUAN, Z., XU, Y., HANG, J., XU, X., LIU, T., GUO, Y., ZENG, W., XIAO, J., GUO, L., LI, X. & MA, W. 2018. Shipping pollution emission associated with increased cardiovascular mortality: A time series study in Guangzhou, China. Environ Pollut, 241, 862-868.

LINDSTAD, H. E., REHN, C. F. & ESKELAND, G. S. 2017. Sulphur abatement globally in maritime shipping. Transportation research. Part D, Transport and Environment, 57, 303-313.

LOHMANN, U. 2006. Aerosol effects on clouds and climate. Space Science Reviews 125, 129-137.

LU, S., ZHANG, H., DU, W. & DENG, J. 2020. Determination of metal elements in workplace air by ICP-MS. MATEC Web of Conferences, 319, 2005.

LV, Z., LIU, H., YING, Q., FU, M., MENG, Z., WANG, Y., WEI, W., GONG, H. & HE, K. 2018. Impacts of shipping emissions on PM2.5 pollution in China. Atmospheric Chemistry and Physics, 18, 15811-15824.

MA, Z., LIU, R., LIU, Y. & BI, J. 2019. Effects of air pollution control policies on PM2.5 pollution improvement in China from 2005 to 2017: a satellite-based perspective. Atmospheric Chemistry and Physics, 19, 6861-6877.

MAHOWALD, N. M., HAMILTON, D. S., MACKEY, K. R. M., MOORE, J. K., BAKER, A. R., SCANZA, R. A. & ZHANG, Y. 2018. Aerosol trace metal leaching and impacts on marine microorganisms. Nature Communications, 9, 2614-15.

MARCH, D., METCALFE K., TINTORE J. & GODLEY B. J. 2021. Tracking the global reduction of marine traffic during the COVID-19 pandemic. Nature Communications 12.

MATTHIAS, V., AULINGER, A., BACKES, A., BIESER, J., GEYER, B., QUANTE, M. & ZERETZKE, M. 2016. The impact of shipping emissions on air pollution in the greater North Sea region – Part 2: Scenarios for 2030. Atmospheric Chemistry and Physics, 16, 759-776.

MATTSON, G. 2006. MARPOL 73/78 and Annex I: An assessment of its effectiveness. Journal of International Wildlife Law and Policy, 9, 175-194.

MAZZEI, F., D'ALESSANDRO, A., LUCARELLI, F., NAVA, S., PRATI, P., VALLI, G. & VECCHI, R. 2008. Characterization of particulate matter sources in an urban environment. Science of The Total Environment, 401, 81-89.

MOHD NOOR, C. W., NOOR, M. M. & MAMAT, R. 2018. Biodiesel as alternative fuel for marine diesel engine applications: A review. Renewable & Sustainable Energy Reviews, 94, 127-142.

NIGAM, A., WELCH, W., MILLER, J. & III, D. R. 2006. Effect of fuel sulphur content and control technology on PM emission from ship's auxiliary engine. Proceeding International Aerosol Conference, 1531-1532.

NORDBERG, G., BERNARD, A., DIAMOND, G. L., DUFFUS, J. H., ILLING, P., NORDBERG, M., BERGDAHL, I. A., JIN, T. & SKERFVING, S. 2018. Risk assessment of effects of cadmium on human health (IUPAC Technical Report). Pure and Applied Chemistry, 90, 755.

O'DOWD, C. D. & DE LEEUW, G. 2007. Marine aerosol production: a review of the current knowledge. PHIL TRANS R SOC A, 365, 1753-1774.

OGUNLAJA, A. S., ALADE, O. S., ODEBUNMI, E. O., MAJAVU, A., TORTO, N. & TSHENTU, Z. R. 2014. The ratios of vanadium-to-nickel and phenanthrene-to-dibenzothiophene as means of identifying petroleum source and classification of Nigeria crude oils. Petroleum Science and Technology, 32, 2283-2291.

OTT, D. K., KUMAR, N. & PETERS, T. M. 2008. Passive sampling to capture spatial variability in PM10-2.5. Atmospheric Environment (1994), 42, 746-756.

ØYVIND, E., EIRIK, S., HANNA LEE, B., PER OLAF, B. & IVAR, S. A. I. 2007. A historical reconstruction of ships' fuel consumption and emissions. Journal of Geophysical Research - Atmospheres, 112, D12301-n/a.

PACYNA, J. M. & PACYNA, E. G. 2001. An assessment of global and regional emissions of trace metals to the atmosphere from anthropogenic sources worldwide. Environmental Reviews, 9, 269-298.

PANDOLFI, M., GONZALEZ-CASTANEDO, Y., ALASTUEY, A., DE LA ROSA, J. D., MANTILLA, E., DE LA CAMPA, A. S., QUEROL, X., PEY, J., AMATO, F. & MORENO, T. 2011. Source apportionment of PM10 and PM2.5 at multiple sites in the strait of Gibraltar by PMF: impact of shipping emissions. Environmental Science and Pollution Research International, 18, 260-269.

PAVESI, T. & MOREIRA, J. C. 2020. Mechanisms and individuality in chromium toxicity in humans. J Appl Toxicol, 40, 1183-1197.

PEY, J., PÉREZ, N., CORTÉS, J., ALASTUEY, A. & QUEROL, X. 2013. Chemical fingerprint and impact of shipping emissions over a western Mediterranean metropolis: Primary and aged contributions. Sci Total Environ, 463-464, 497-507.

PIRJOLA, L., PAJUNOJA, A., WALDEN, J., JALKANEN, J. P., RÖNKKÖ, T., KOUSA, A. & KOSKENTALO, T. 2014. Mobile measurements of ship emissions in two harbour areas in Finland. Atmospheric Measurement Techniques, 7, 149-161.

PLATTS, S. P. G. 2021. Bunker price indices in container transportation webinar.

PROSPERO, J. M. 2002. The chemical and physical properties of marine aerosols: An introduction.

QIAN, Y., BEHRENS, P., TUKKER, A., RODRIGUES, J. F. D., LI, P. & SCHERER, L. 2019. Environmental responsibility for sulfur dioxide emissions and associated biodiversity loss across Chinese provinces. Environ Pollut, 245, 898-908.

QIN, Z., YIN, J. & CAO, Z. 2017. Evaluation of effects of ship emissions control areas: Case study of Shanghai Port in China. Transportation Research Record, 2611, 50-55.

QUEROL, X. 2001. PM10 and PM2.5 source apportionment in the Barcelona Metropolitan area, Catalonia, Spain. Atmospheric environment (1994), 35, 6407-6419.

ROSSER, F., FORNO E., KURLAND S. K., HAN Y. Y., MAIR C., ACOSTA-PEREZ C., CANINO G. & CELEDON J. C. 2020. Annual SO2 exposure, asthma, atopy, and lung function in Puerto Rican children. Pediatric Pulmonology 55, 330-337.

RUDICH, Y., KAUFMAN, Y. J., DAYAN, U., HONGBIN, Y. & KLEIDMAN, R. G. 2008. Estimation of transboundary transport of pollution aerosols by remote sensing in the eastern Mediterranean. Journal of Geophysical Research - Atmospheres, 113, D14S13-n/a.

SALTZMAN, E. S. 2009. Marine Aerosols.

SARAÇOĞLU, H., DENIZ, C. & KıLıÇ, A. 2013. An investigation on the effects of ship sourced emissions in Izmir Port, Turkey. Scientific World Journal, 2013, 218324-8.

SCHULZE, B. C., WALLACE, H. W., BUI, A. T., FLYNN, J. H., ERICKSON, M. H., ALVAREZ, S., DAI, Q., USENKO, S., SHEESLEY, R. J. & GRIFFIN, R. J. 2018. The impacts of regional shipping emissions on the chemical characteristics of coastal submicron aerosols near Houston, TX. Atmospheric Chemistry and Physics, 18, 14217-14241.

SERGEY, U. & NICOLAS, L. 2019. Assessment of hydrotreated vegetable oil (HVO) applicability as an alternative marine fuel based on its performance and emissions characteristics. SAE International Journal of Fuels and Lubricants, 12, 109-120.

SOEROSO, N. N., ITAN T. K. & ICHWAN M., T. K. 2019. Factors associated decrease of forced vital capacity on gas station employees exposed to sulfur dioxide (SO2). IOP Conference Series: Earth and Environmental Science 245, 012015.

SOFIEV, M., WINEBRAKE, J. J., JOHANSSON, L., CARR, E. W., PRANK, M., SOARES, J., VIRA, J., KOUZNETSOV, R., JALKANEN, J.-P. & CORBETT, J. J. 2018. Cleaner fuels for ships provide public health benefits with climate tradeoffs. Nat Commun, 9, 406-406.

SPADA, N. J., CHENG, X., WHITE, W. H. & HYSLOP, N. P. 2018. Decreasing vanadium footprint of bunker fuel emissions. Environ. Sci. Technol, 52, 11528-11534.

STATISTA 2021. Global marine bunkers product demand in 2018 with a forecast for 2019 to 2024, by fuel type.

STEIN, A. F., DRAXLER, R. R., ROLPH, G. D., STUNDER, B. J. B., COHEN, M. D. & NGAN, F. 2015. NOAA's HYSPLIT atmospheric transport and dispersion modelling system. Bulletin of the American Meteorological Society, 96, 2059-2078.

STREETS, D. G., CARMICHAEL, G. R. & ARNDT, R. L. 1997. Sulfur dioxide emissions and sulfur deposition from international shipping in Asian waters. Atmospheric Environment (1994), 31, 1573-1582.

SVENSSON, E. 2011. The Regulation of global SOx emissions from ships: IMO proceedings 1988-2008.

TAO, L., FAIRLEY, D., KLEEMAN, M. J. & HARLEY, R. A. 2013. Effects of switching to lower sulfur marine fuel oil on air quality in the San Francisco Bay Area. Environ. Sci. Technol, 47, 10171-10178.

TAYLOR, R. & MCLENNAN, S. M. 1995. The geochemical evolution of the continental crust. Reviews of Geophysics, 33, 241-265.

THOMAS, G. B., FRANCES, E. H., PIERRE, W. C., PHILIP, D. N., MARGARET, J. Y., ROBIN, W. P., IAN, M. B. & TIMOTHY, J. S. 2016. Air-sea fluxes of CO2 and CH4 from the Penlee Point Atmospheric Observatory on the south-west coast of the UK. Atmospheric Chemistry and Physics, 16, 5745-5761.

TOLOCKA, M. P., SOLOMON, P. A., MITCHELL, W., NORRIS, G. A., GEMMILL, D. B., WIENER, R. W., VANDERPOOL, R. W., HOMOLYA, J. B. & RICE, J. 2001. East versus West in the US: Chemical Characteristics of PM2.5 during the Winter of 1999. Aerosol Science and Technology, 34, 88-96.

TOMLINSON, G. H. 1983. Air pollutants and forest decline. Environ. Sci. Technol, 17, 246A-256A.

TUNNICLIFFE, W. S., HILTON, M. F., HARRISON, R. M. & AYRES, J. G. 2001. The effect of sulphur dioxide exposure on indices of heart rate variability in normal and asthmatic adults. European Respiratory Journal, 17, 604-608.

UHER, G. 2006. Distribution and air–sea exchange of reduced sulphur gases in European coastal waters. Estuarine, Coastal and Shelf science, 70, 338-360.

VIANA, M., AMATO, F., ALASTUEY, A., QUEROL, X., MORENO, T., GARCÍA DOS SANTOS, S., HERCE, M. D. & FERNÁNDEZ-PATIER, R. 2009a. Chemical tracers of particulate emissions from commercial shipping. Environmental Science & Technology, 43, 7472-7477.

VIANA, M., AMATO, F., ALASTUEY, A. S., QUEROL, X., MORENO, T., GARCÍA DOS SANTOS, S. L., HERCE, M. A. D. & FERNÁNDEZ-PATIER, R. A. 2009b. Chemical

tracers of particulate emissions from commercial shipping. Environ. Sci. Technol, 43, 7472-7477.

VISSCHEDIJK, A. H. J., DENIER VAN DER GON, H. A. C., HULSKOTTE, J. H. J. & QUASS, U. 2013. Anthropogenic vanadium emissions to air and ambient air concentrations in North-West Europe. E3S Web of Conferences, 1, 3004.

VUČKOVIĆ, I., ŠPIRIĆ, Z., STAFILOV, T., KUŠAN, V. & BAČEVA, K. 2013. The study on air pollution with nickel and vanadium in Croatia by using moss biomonitoring and ICP-AES. Bull Environ Contam Toxicol, 91, 481-487.

WANG, Z., PAULAUSKIENE, T., UEBE, J. & BUCAS, M. 2020. Characterization of Biomethanol-Biodiesel-Diesel blends as alternative fuel for marine Applications. Journal of Marine Science and Engineering, 8, 730.

WHITE, C., USSHER, S. J., FITZSIMONS, M. F., ATKINSON, S., WOODWARD, E. M. S., YANG, M. & BELL, T. G. 2021. Inorganic nitrogen and phosphorus in Western European aerosol and the significance of dry deposition flux into stratified shelf waters. Atmospheric Environment (1994), 261, 118391.

WHO 2000. Vanadium, second edition. Air Quality Guidelines.

WYSOCKA, I. 2021. Determination of rare earth elements concentrations in natural waters – A review of ICP-MS measurement approaches. Talanta (Oxford), 221, 121636-121636.

XIAO, Q., LI, M., LIU, H., FU, M., DENG, F., LV, Z., MAN, H., JIN, X., LIU, S. & HE, K. 2018. Characteristics of marine shipping emissions at berth: profiles for particulate matter and volatile organic compounds. Atmospheric Chemistry and Physics, 18, 9527-9545.

XIE, X., WANG Y.Y., LYU G., ZHOU G.Q., CHENG T. T., LIU Y. H., PENG Y. R., HE Q. S., GAO W., LI X. & ZHANG Q. 2019. Effects of shipping-originated aerosols on physical cloud properties over marine areas near East China." Aerosol and Air Quality Research 19, 1471-1482.

YAKUBOV, M. R., MILORDOV, D. V., YAKUBOVA, S. G., BORISOV, D. N., IVANOV, V. T. & SINYASHIN, K. O. 2016. Concentrations of vanadium and nickel and their ratio in heavy oil asphaltenes. Petroleum Chemistry, 56, 16-20.

YANG, M., BELL, T. G., HOPKINS, F. E., KITIDIS, V., CAZENAVE, P. W., NIGHTINGALE, P. D., YELLAND, M. J., PASCAL, R. W., PRYTHERCH, J., BROOKS, I. M. & SMYTH, T. J. 2016a. Air-sea fluxes of CO2 and CH4 from the Penlee Point Atmospheric Observatory on the south-west coast of the UK. Atmospheric Chemistry and Physics, 16, 5745.

YANG, M., BELL, T. G., HOPKINS, F. E. & SMYTH, T. J. 2016b. Attribution of atmospheric sulfur dioxide over the English Channel to dimethyl sulfide and changing ship emissions. Atmospheric Chemistry and Physics, 16, 4771-4783.

YANG, M., BELL, T. G., HOPKINS, F. E. & SMYTH, T. J. 2016c. Attribution of Atmospheric Sulfur Dioxide over the English Channel to Dimethylsulfide and Changing Ship Emissions. Atmospheric Chemistry and Physics, 16, 1.

YANG, M., NORRIS, S. J., BELL, T. G. & BROOKS, I. M. 2019. Sea spray fluxes from the southwest coast of the United Kingdom – dependence on wind speed and wave height. Atmospheric Chemistry and Physics, 19, 15271-15284.

YANG, W. & OMAYE, S. T. 2009. Air pollutants, oxidative stress and human health. Mutation research. Genetic Toxicology and Environmental Mutagenesis, 674, 45-54.

YEELES, A. 2018. Shipping emissions. Nature Climate Change, 8, 457-457.

YU, G., ZHANG, Y., YANG, F., HE, B., ZHANG, C., ZOU, Z., YANG, X., LI, N. & CHEN, J. 2021. Dynamic Ni/V ratio in the ship-emitted particles driven by multiphase Fuel oil regulations in coastal China. Anthropogenic Impact on the Atmosphere.

YUN, J., ZHU, C., WANG, Q., HU, Q. & YANG, G. 2019. Catalytic conversions of atmospheric sulfur dioxide and formation of acid rain over mineral dusts: Molecular oxygen as the oxygen source. Chemosphere, 217, 18-25.

ZETTERDAHL, M., MOLDANOVÁ, J., PEI, X., PATHAK, R. K. & DEMIRDJIAN, B. 2016. Impact of the 0.1% fuel sulfur content limit in SECA on particle and gaseous emissions from marine vessels. Atmospheric Environment (1994), 145, 338-345.

ZHANG, F., CHEN, Y., TIAN, C., WANG, X., HUANG, G., FANG, Y. & ZONG, Z. 2014. Identification and quantification of shipping emissions in Bohai Rim, China. Sci Total Environ, 497-498, 570-577.

ZHANG, X., ZHANG, Y., LIU, Y., ZHAO, J., ZHOU, Y., WANG, X., YANG, X., ZOU, Z., ZHANG, C., FU, Q., XU, J., GAO, W., LI, N. & CHEN, J. 2019. Changes in the SO2 Level and PM2.5 Components in Shanghai driven by implementing the Ship Emission Control Policy. Environ. Sci. Technol, 53, 11580-11587.

ZHAO, J., ZHANG, Y., XU, H., TAO, S., WANG, R., YU, Q., CHEN, Y., ZOU, Z. & MA, W. 2021. Trace elements from ocean-going vessels in East Asia: Vanadium and Nickel emissions and their impacts on air quality. Journal of geophysical research. Atmospheres, 126, n/a.

ZHAO, M., ZHANG, Y., MA, W., FU, Q., YANG, X., LI, C., ZHOU, B., YU, Q. & CHEN, L. 2013. Characteristics and ship traffic source identification of air pollutants in China's largest port. Atmospheric Environment (1994), 64, 277-286.
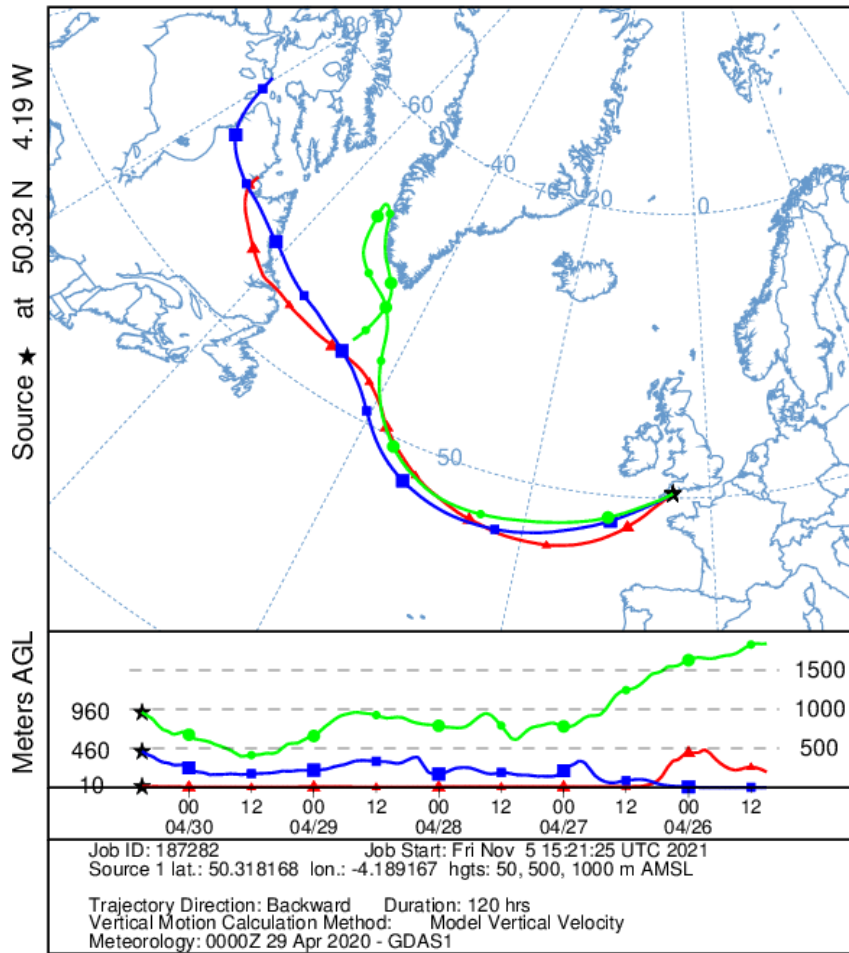
Appendix

Figure A1. Example of HYSPLIT back trajectory classed as a Clean Marine air mass.

NOAA HYSPLIT MODEL
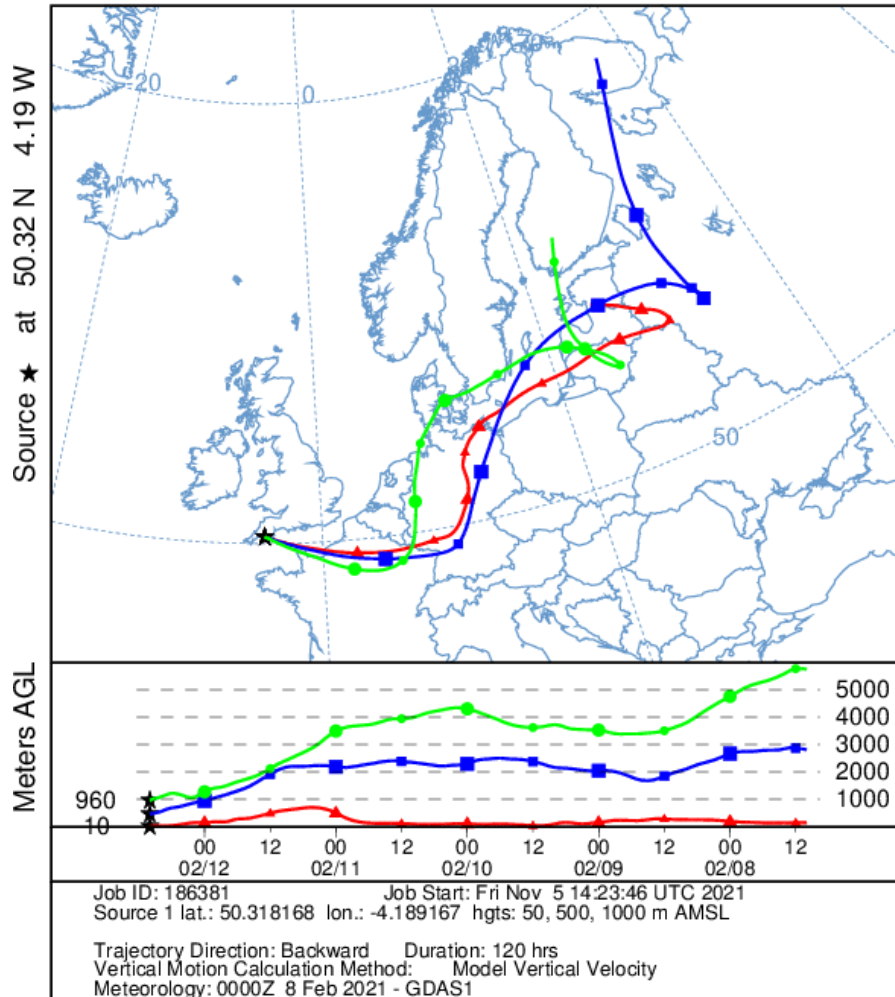Backward trajectories ending at 1000 UTC 12 Feb 21
GDAS Meteorological Data

Source ★ at 50.32 N 4.19 W

Meters AGL

Job ID: 186381   Job Start: Fri Nov 5 14:23:46 UTC 2021
Source 1 lat.: 50.318168 lon.: -4.189167 hgts: 50, 500, 1000 m AMSL

Trajectory Direction: Backward   Duration: 120 hrs
Vertical Motion Calculation Method: Model Vertical Velocity
Meteorology: 0000Z 8 Feb 2021 - GDAS1

Figure A2. Example of HYSPLIT back trajectory classed as a Central European air mass.
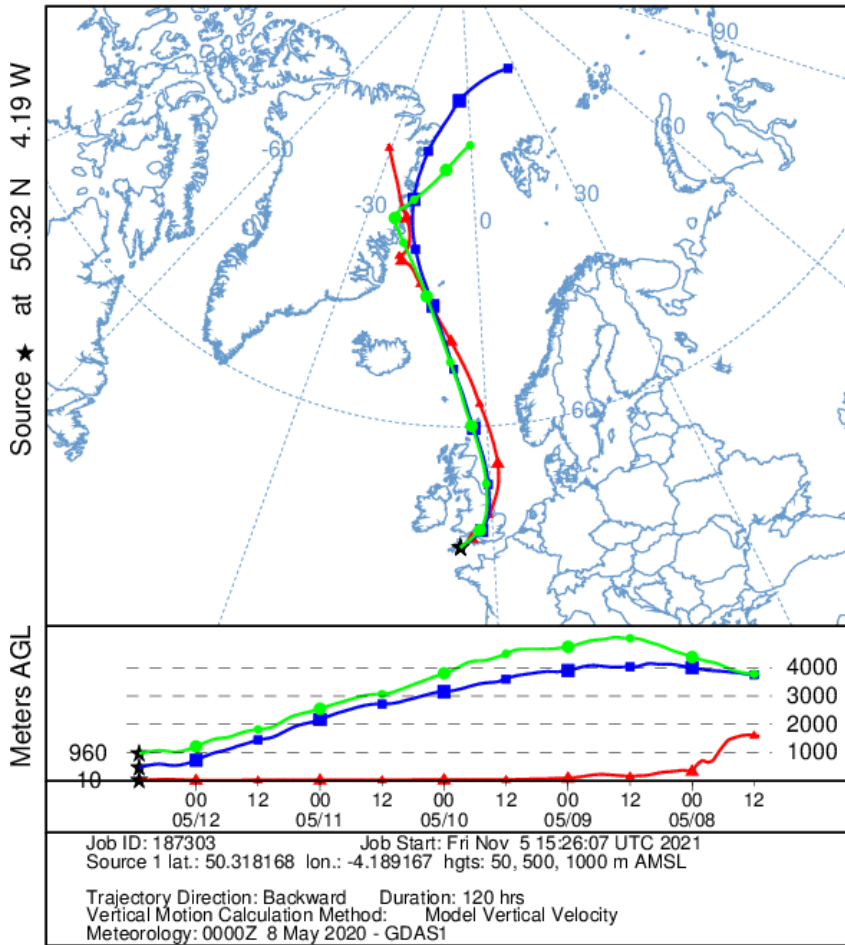
Figure A3. Example of HYSPLIT back trajectory classed as a Mainland UK/Ireland
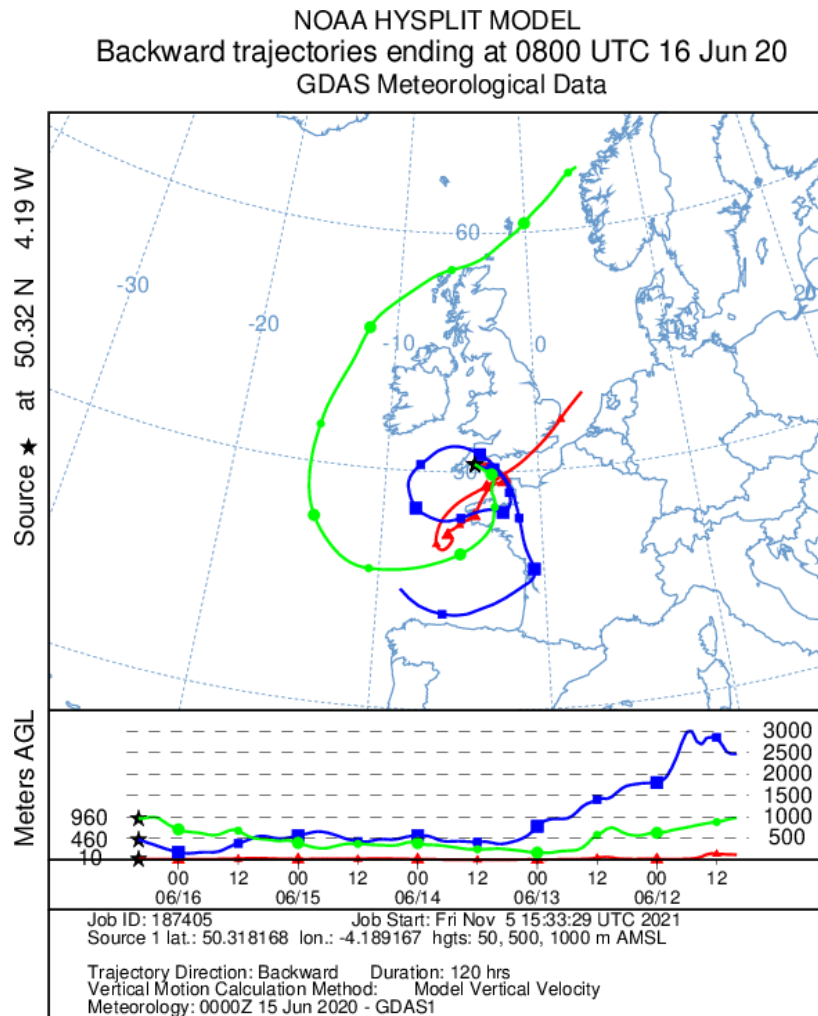
Figure A4. Example of HYSPLIT back trajectory classed as an Unregulated Shipping air
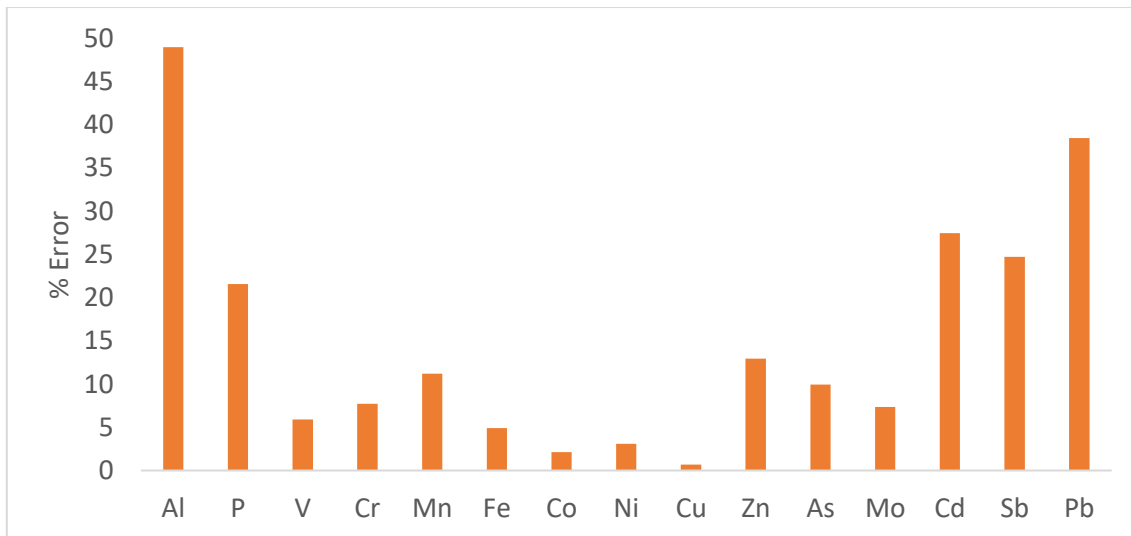
mass.

Figure A5. Error from ICP-MS analysis of the certified reference material (EP-L)